



**NEAR EAST UNIVERSITY**

**INSTITUTE OF GRADUATE STUDIES**

**DEPARTMENT OF ANALYTICAL CHEMISTRY**

**DETERMINATION OF ACIDITY CONSTANT VALUES AND  
ELECTROCHEMICAL REDUCTION MECHANISM OF SOME  
COUMARIN DERIVATIVES**

**Ph.D. THESIS**

**Semra ALTUNTERİM**

**Nicosia**

**December, 2021**

**NEAR EAST UNIVERSITY**  
**INSTITUTE OF GRADUATE STUDIES**  
**DEPARTMENT OF ANALYTICAL CHEMISTRY**

**DETERMINATION OF ACIDITY CONSTANT VALUES AND  
ELECTROCHEMICAL REDUCTION MECHANISM OF SOME  
COUMARIN DERIVATIVES**

**Ph. D. THESIS**

**Semra ALTUNTERİM**

**Supervisor**



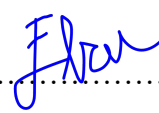
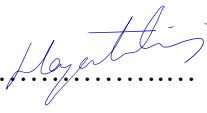
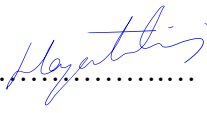
**Assoc. Prof. Hayati ÇELİK**

**Nicosia**

**December, 2021**

## Approval

We certify that we have read the thesis submitted by Semra Altunterim titled “**Determination of Acidity Constant Values and Electrochemical Reduction Mechanism of Some Coumarin Derivatives**” and that in our combined opinion it is fully adequate, in scope and in quality, as a thesis for the degree of Doctor of Science.

Examining Committee	Name-Surname	Signature
Head of the Committee:	Prof. Dr. Şahan SAYGI	..... 
Committee Member:	Assoc. Prof. Soner ÇUBUK	..... 
Committee Member:	Assist. Prof. Selin IŞIK	..... 
Committee Member:	Assist. Prof. Ebru TÜRKÖZ ACAR	..... 
Supervisor:	Assoc. Prof. Dr. Hayati ÇELİK	..... 

Approved by the Head  
of the Department

...../...../.....

**Assist. Prof. Selin  
Işık**

**Head of  
Department**

Approved by the  
Institute of Graduate  
Studies

...../...../.....

**Prof. Dr. Kemal  
Hüsnü Can Başer**

**Head of the  
Institute**

**Declaration**

I hereby declare that all information, documents, analysis and results in this thesis have been collected and presented according to the academic rules and ethical guidelines of Institute of Graduate Studies, Near East University. I also declare that as required by these rules and conduct, I have fully cited and referenced information and data that are not original to this study.

**Semra Altunterim**

**28/12/2021**

## **Acknowledgments**

First and foremost, I sincerely thank my supervisor, Assoc. Prof. Hayati Çelik, who had supported me with sharing his great experience, and had helped me every process for my work.

I appreciate to Prof. Dr. Şahan Saygı from Near East University, Assoc. Prof. Dr. Soner Çubuk from Marmara University, Assist. Prof. Ebru Türköz Acar from Yeditepe University and Assist. Prof. Selin Işık from Near East University for being my jury member. Also, I thank to all the members of the faculty of pharmacy at Near East University.

Also special thanks to Assoc. Prof. Melek Şirin Çelik from Marmara University for helping me during my thesis.

I would also like to thank my mother, Ayten Altunterim and my parents for their helps, love and endless patience in my motivation.

Finally, I would like to thank my husband, Özgür Erkan, who was always there cheering me up and stood by me through the good and bad times.

**Semra Altunterim**

**Abstract****Determination of Acidity Constant Values and Electrochemical Reduction  
Mechanism of Some Coumarin Derivatives****Altuntemir, Semra****Ph.D, Department of Analytical Chemistry****Supervisor: Assoc. Prof. Hayati ÇELİK****December 2021, 91 pages**

Firstly, the acid dissociation constant values of newly synthesized some coumarin derivatives were determined by UV–VIS spectrophotometry and/or potentiometric methods in this study and the obtained values were compared with theoretical  $pK_a$  values. The studied compounds were of two kinds; compounds in one group contained piperazine ring whereas others contained piperidine ring. As a result of the observations, reaction schemes for both piperazine and piperidine derivatives were proposed. The agreement between the experimentally and theoretically determined  $pK_a$  values was significant for most of the compounds and for the others a correlation between their substituents and unexpected behavior is made based on the differences in their acidities. Anti-inflammatory effects of these compounds were related with their acidity and structures. Even though a clear conclusion could not be made on the anti-inflammatory effect-structure relationship for the studied compounds, aryl-substituted piperazine heterocycle bearing compounds was suggested for the development of new drug candidates with possible anti-inflammatory effects.

Finally, electrochemical reduction mechanism of coumarin derivatives containing piperidine and piperazine substituents have been studied in this thesis. The behavior of these two groups follows two different way of electron transfer. However, the same group has been reduced for both group of compounds. For piperidine derivatives, the reduction occurs on the carbon-carbon double bond on the coumarin ring. This reduction depends on the acidity of the solution. It has been

shown that before electron uptakes, hydrogen ions transfer first on the coumarin ring due to the dependence of half-wave potentials on pHs. For piperazine derivatives, the reduction occurs on the carbon-carbon double bond on the coumarin ring as piperidine derivatives. This reduction does not depend on the acidity of the solution. It has been shown that half-wave potentials are independent of acidity of the solution. Therefore, before hydrogen ions transfer, first electron uptakes on the coumarin ring due to the independence of half-wave potentials on pHs. Reduction mechanisms of coumarin derivatives have been suggested for studied compounds.

**Keywords:** Coumarin, acid dissociation constant, spectrophotometry, potentiometry, electrochemical reduction

## Özet

### Bazı Kumarin Türevlerinin Asitlik Sabit Değerleri ve Elektrokimyasal İndirgeme Mekanizmalarının Belirlenmesi

Altunterim, Semra

Doktora, Analitik Kimya Anabilim Dalı

Danışman: Doç. Dr. Hayati ÇELİK

Aralık, 2021, 91 sayfa

Bu çalışmada ilk olarak yeni sentezlenen bazı kumarin türevlerinin asit ayrışma sabiti değerleri UV-VIS spektrofotometresi ve/veya potansiyometrik yöntemlerle belirlenmiş ve elde edilen değerler teorik  $pK_a$  değerleri ile karşılaştırılmıştır. Çalışılan bileşiklerin bir kısmı piperazin halkası diğer grup piperidin halkası içeriyor. Gözlemler sonucu hem piperazin hem de piperidin türevleri için reaksiyon mekanizmaları önerildi. Deneysel ve teorik olarak belirlenen  $pK_a$  değerleri arasındaki uyum, bileşiklerin çoğu için önemliydi ve asitliklerindeki farklılıklara bağlı olarak, sübstitüentleri ve beklenmedik davranışlar arasında bir korelasyon yapıldı. Bu bileşiklerin antiinflamatuvar etkileri, asitlikleri ve yapıları ile ilişkilidir. Çalışılan bileşikler için anti-inflamatuvar etki-yapı ilişkisi hakkında net bir sonuca varılamasa da olası anti-inflamatuvar etkileri olan yeni ilaç adaylarının geliştirilmesi için aril-sübstitüe edilmiş piperazin heterosiklik türevler önerilmiştir.

Son olarak, tezde piperidin ve piperazin sübstitüentleri içeren kumarin türevlerinin elektrokimyasal indirgenme mekanizması incelenmiştir. Bu iki grupta  $e^-$  transferi iki farklı yol izler. Her iki bileşik grubunda aynı grup indirgenmiştir. Piperidin türevleri için indirgeme, kumarin halkası üzerindeki çift karbon-karbon bağında meydana gelir. Bu indirgenme, çözeltinin asitliğine bağlıdır. Elektron alımından önce, yarı dalga potansiyellerinin pH'lara bağımlılığından dolayı ilk olarak hidrojen iyonlarının kumarin halkasından transfer olduğu gösterilmiştir. Piperazin türevleri için indirgenme, piperidin türevleri gibi kumarin halkası üzerindeki karbon-karbon çift bağında meydana gelir. Bu indirgenme, çözeltinin asitliğine bağlı değildir. Yarı dalga potansiyellerinin, çözeltinin asitliğinden bağımsız olduğu gösterilmiştir. Yarı dalga potansiyellerinin pH' dan bağımsız olması sebebiyle



kumarin halkasında ilk olarak elektron alımı gerçekleşir. Çalışılan kumarin türevlerinin indirgeme mekanizmaları önerilmiştir.

**Anahtar kelimeler:** kumarin, asit ayrışma sabiti, spektrofotometri, potansiyometri, elektrokimyasal indirgeme

## Contents

Approval .....	I
Declaration .....	II
Acknowledgments .....	III
Abstract .....	IV
Özet .....	VI
Contents .....	VIII
List of Figures .....	X
List of Tables .....	XII
Abbreviations .....	XIII
<b>CHAPTER I .....</b>	<b>1</b>
Introduction .....	1
General Information of Coumarines .....	1
Ionization Constant Values of Coumarin Derivatives .....	3
Polarography .....	10
Polarographic methods .....	15
Undesired conditions in polarography .....	16
Types of Mercury Electrodes Used in Polarography .....	17
<b>CHAPTER II .....</b>	<b>21</b>
Literature Review .....	21
Coumarins .....	21
Photophysical and Photochemical Properties of Coumarins .....	21
Biological and Physiological Activities of Coumarins .....	22
Determination of Ionization constants of Coumarins .....	22
Determination of Reduction of Coumarins .....	23
<b>CHAPTER III .....</b>	<b>25</b>
Methodology .....	25
Ionization Constant Assignment Methods .....	25
Methods And Calculations .....	31
Polarography method .....	32
<b>CHAPTER IV .....</b>	<b>34</b>
Findings and Discussion .....	34
Determination of Ionization Constants .....	34
Polarography .....	44

CHAPTER V.....	66
Discussion .....	66
Determination of Ionization Constants .....	66
Polarography .....	66
CHAPTER VI.....	70
Conclusion and Recommendations .....	70
Determination of Ionization Constants .....	70
Polarography .....	71
REFERENCES.....	73

## List of Figures

Figure 1. Structures of Coumarins .....	2
Figure 2. Single Beam Schematic Diagram .....	7
Figure 3. Double Beam Schematic Diagram.....	7
Figure 4. Electronic Transitions.....	8
Figure 5. Classical Design of The Dropping Mercury Electrode.....	11
Figure 6. Polarograms for A, a 1 M solution of HCl that is $5 \times 10^{-4}$ in $Cd^{+2}$ and B, a 1M solution of HCl .....	13
Figure 7. Types of Electrodes used in Polarography (a) Hanging Mercury Drop Electrode (b) Dropping Mercury Electrode (c) Static Mercury Drop Electrode .....	18
Figure 8. Standard Sample Cuvette with a Path Length of 1 cm .....	25
Figure 9. Spectra of a Substance at Different pH Values and Plotting the pH-Absorbance Graph.....	27
Figure 10. Potentiometric Titration Curves .....	28
Figure 11. Schematic Diagram of Glass Electrode .....	29
Figure 12. Amount of Added Base (NaOH) as a Function of pH for Compound 2 ...	35
Figure 13. Acid-Base Equilibria of Compounds 2-16 .....	36
Figure 14. Absorbance vs Wavelength plot for $5 \times 10^{-5}$ M Compound 2 in Various Buffered Solutions. pH Values: (a) 4.74, (b) 5.20, (c) 5.70, (d) 6.20, (e) 6.75, (f) 7.25, (g) 7.60, (h) 8.25, (i) 8.40, (j) 8.65 and (k) 8.80. ....	37
Figure 15. Absorbance vs Wavelength Plot for $5 \times 10^{-5}$ M Compound 20 in Various Buffered Solutions. pH Values: (a) 4.80, (b) 5.15, (c) 5.65, (d) 5.80, (e) 6.30, (f) 6.80, (g) 7.25, (h) 8.75, (i) 9.30, and (j) 9.90. ....	40
Figure 16. Acid-Base Equilibria of Compounds 17-24 .....	41
Figure 17. Absorbance vs Wavelength Plot for $5 \times 10^{-5}$ M Compound 22 in Various Buffered Solutions. pH Values: (a) 5.26, (b) 5.80, (c) 6.28, (d) 6.80, (e) 7.32, (f) 7.80, (g) 8.30, (h) 8.75, (i) 9.30, (j) 9.80, (k) 10.00 and (l) 10.25.....	41
Figure 18. Amount of Added Base (NaOH) As a Function of pH for Compound 22. 42	
Figure 19. Current-Voltage Plot of Compound 18. pH values: pH 3.85, pH 4.75, pH 5.75, pH 6.22, pH 6.70, pH 7.25, pH 7.70, pH 8.25, pH 8.80, pH 9.30, pH 9.75, pH 10.25.....	45
Figure 20. $E_{1/2}$ -pH Plot of Compound 18: pH 6.70, pH 7.25, pH 7.70, pH 8.25, pH 8.80.....	46
Figure 21. Current-Voltage Plot of Compound 25. pH Values: pH 7.70, pH 8.25, pH 8.80, pH 9.25.....	47
Figure 22. Current-Voltage Plot of Compound 22. pH Values: pH 6.70, pH 7.70, pH 8.25, pH 8.80.....	48
Figure 23. $E_{1/2}$ -pH Plot of Compound 22: pH 6.70, pH 7.70, pH 8.25, pH 8.80.....	49
Figure 24. Current-Voltage Plot of Compound 17. pH Values: pH 7.25, pH 7.70, pH 8.25, pH 8.80.....	50
Figure 25. $E_{1/2}$ -pH Plot of Compound 17: pH 7.25, pH 7.70, pH 8.25, pH 8.80.....	50
Figure 26. Current-Voltage Plot of Compound 24. pH Values: pH 6.70, pH 7.25, pH 7.70, pH 8.25, pH 8.80.....	51
Figure 27. $E_{1/2}$ -pH Plot of Compound 24: pH 6.70, pH 7.25, pH 7.70, pH 8.25, pH 8.80.....	52

Figure 28. Electrochemical Reduction Mechanism of Piperidine Derivatives.....	53
Figure 29. Current-Voltage Plot of Compound 2. pH values: pH 7.70, pH 8.25, pH 8.80, pH 9.25, pH 9.75.....	54
Figure 30. $E_{1/2}$ -pH Plot of Compound 2: pH 7.70, pH 8.25, pH 8.80, pH 9.25, pH 9.75.....	55
Figure 31. Current-Voltage Plot of Compound 8. pH values: pH 6.70, pH 7.25, pH 7.70, pH 8.25, pH 8.80.....	56
Figure 32. $E_{1/2}$ -pH Plot of Compound 8: pH 6.70, pH 7.25, pH 7.70, pH 8.25.....	57
Figure 33. Current-Voltage Plot of Compound 9. pH Values: pH 6.70, pH 7.25, pH 7.70, pH 8.25, pH 8.80.....	58
Figure 34. $E_{1/2}$ -pH Plot of Compound 9: pH 6.70, pH 7.25, pH 7.70, pH 8.25.....	59
Figure 35. Current-Voltage Plot of Compound 10. pH values: pH 6.70, pH 7.25, pH 7.70, pH 8.25, pH 8.80, pH 9.25.....	60
Figure 36. $E_{1/2}$ -pH Plot of Compound 10: pH 6.70, pH 7.25, pH 7.70, pH 8.25, pH 8.80, pH 9.25.....	60
Figure 37. Current-Voltage Plot of Compound 15. pH Values: pH 5,80, pH 6,22, pH 6.70, pH 7.25, pH 7.70, pH 8.25, pH 8.80 pH 9,25.....	61
Figure 38. $I-h^{1/2}$ Plot of Compound 11.....	62
Figure 39. Plot of $i$ vs $h$ (a) and $i$ vs $h^{1/2}$ (b) for Compound 12.....	63
Figure 40. Plot of Current vs Concentration for Compound 12.....	64
Figure 41. Electrochemical Reduction Mechanism of Piperazin Derivatives.....	65
Figure 42. Reduction Mechanism of Coumarin.....	68
Figure 43. Possible Mechanism of Coumarin.....	69

**List of Tables**

Table 1. Electronic Transition Involving $n$ , $\sigma$ and $\pi$ Molecular Orbitals .....	9
Table 2. List of Compounds Studied .....	30
Table 3. Experimental and Theoretically Calculated pKa Values of Compounds 1-13. .....	34
Table 4. Experimentally and Theoretically Calculated pKa Values of Compounds 17- 24.....	38
Table 5. Theoretical pKa Values for 6th Position Hydroxyl Derivatives Together with the Studied Compounds. ....	43

**List of Abbreviations**

<b>A</b>	Absorbance
<b>K<sub>a</sub></b>	Acid dissociation constant
<b>K<sub>b</sub></b>	Base dissociation constant
<b>C</b>	Concentration
<b>I</b>	Ionic strength
<b>λ</b>	Wavelength
<b>b</b>	Path length
<b>π</b>	Pi bond
<b>P</b>	Poker
<b>σ</b>	Sigma bond
<b>T</b>	Transmittance
<b>UV</b>	Ultraviolet
<b>VIS</b>	Visible
<b>SCE</b>	Saturated calomel electrode
<b>E<sub>1/2</sub></b>	Half potential
<b>I</b>	Current
<b>SMDE</b>	Static Mercury Drop Electrode
<b>DME</b>	Dropping Mercury Electrode
<b>DCP</b>	Direct Current Polarography
<b>HDME</b>	Hanging Mercury Drop Electrode
<b>CV</b>	Cyclic Voltammetry

## CHAPTER I

### Introduction

#### General Information of Coumarines

As a result of condensation of the pyron ring with the benzene ring, a class of heterocyclic compounds known as benzopyrans are formed, this heterocyclic structure is called coumarin. Coumarin, the main compound of the benzo- $\alpha$ -pyrone group, was first isolated by VOGEL in 1820 from the fragrant seeds of a tree called Tonka bean (semen tonka) and *Dipteryx odorato* (Aubl.) Willd. (Coumarouna odorato) from the Fabaceae family. It was named coumarin because it was first isolated from this compound (Sethna & Shah, 1945).

Coumarin derivatives, which were synthesized for the first time by the Perkin method, can also be synthesized by other methods such as Pechmann, Knoevenagel, or Wittig methods. Ordinarily, colorless coumarin compounds can be converted to colored dyes by linking different substituted groups to the coumarin ring (Buran et al., 2019; Peng, LV Damu, & Zhou, 2013). In addition to the coloring effect, depending on the location of the substituents, different characteristics of this class of compounds are observed. Coumarin derivatives, particularly due to the diversity of their biological activity such as antimicrobial (Peng et al., 2013), anticoagulant (Golfakhrabadi et al., 2014), anti-inflammatory (Luchini et al., 2008), anticancer (Nasr, et al., 2014), and antidepressant (Abdel-Latif, 2005) properties, are commonly used in the drug industry. Furthermore, coumarins can be used as industrial additives in perfumes, cosmetics, and tobaccos (Fais et al., 2009; Matos et al., 2013). Given the great potential of this chemical structure and the limited number of studies that focus on molecules that are derived by substituting on the 8<sup>th</sup> carbon of the benzopyran ring, some aromatic and aliphatically substituted piperidine and piperazines were evaluated for their anti-inflammatory activity, analgesic activity and cytotoxicity and new molecules were synthesized. According to the results, it was shown that some of the compounds yielded anti-inflammatory activities in vitro study. Additionally, some of them also demonstrated analgesic activities with low cytotoxicity (Buran et al., 2019).

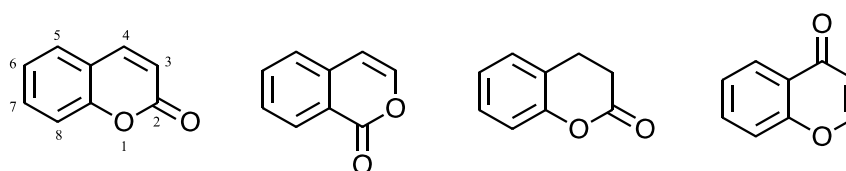
IUPAC name of Coumarin is 2*H*-1-benzopyran-2-one or chromen-2-one. Moreover, coumarins, chroman and chromones belong to the same chemical family



(Figure.1). Coumarins are conjugated compounds and they can be characterized with UV-spectrophotometry. In UV, their blue fluorescent is a distinct feature.

Figure 1.

*Structures of Coumarins*



Coumarin

Isocoumarin

Chroman

Chromone

(*2H-1-benzopyran-2-one*) (*1H-2-benzopyran-1-one*) (*4H-1-benzopyran-4-one*)

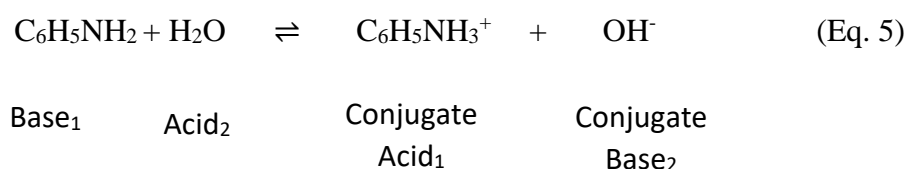
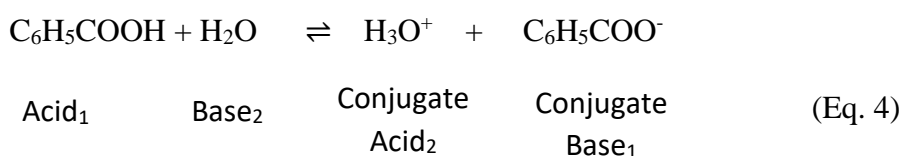
The synthesis of these coumarin derivatives made by Kerem Buran et al. is given below. Resorcinol was dissolved in concentrated sulfuric acid at 0 °C, then ethyl acetoacetate (e.q 1) was added and the mixture was stirred at 0-5 °C for 2 hours. Then the reaction mixture was poured onto ice-water. After that the solid was washed with water and recrystallized from ethanol. Finally, pure white solid 7-Hydroxy-4-methyl-chromen-2-one was obtained (e.q 1). Compound **1** (7-Hydroxy-4-methyl-chromen-2-one;) was dissolved in 95% ethanol, then piperazine derivative(s) ( $R_1$ ) and formaldehyde were added to the reaction medium. The reaction mixture was refluxed for 4-6 hours. At the end of the 4-6 hours, the reaction medium was cooled, then the solvent was evaporated in *vacuo*. Pale-yellow oils were obtained and further treated with a little amount of cool acetone. Then, the white solids were crystallized from acetone. (e.q 2)

Compound **1** (7-Hydroxy-4-methyl-chromen-2-one) was dissolved in 95% ethanol, then piperazine derivative(s) ( $R_2$ ) and formaldehyde were added to the reaction medium. The reaction mixture was refluxed for 4-6 hours. At the end of the 4-6 hours, the reaction medium was cooled, then the solvent was evaporated in *vacuo*. Pale-yellow oils were obtained and further treated with a little amount of cool acetone. Then, the white solids were crystallized from acetone (e.q 3) (Buran, et al., 2021) .



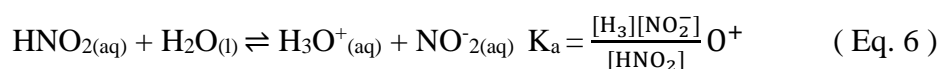
are named as base, while substances that can accept an electron pair from the base to form a covalent bond are named as acid.

Acids and bases that are related by mutual exchange of protons are called conjugated acid-base pairs. That is, the new type of proton formed by the ionization of the acid in the environment tends to take up and this is called the conjugate base of that acid. Similarly, the new type formed by some taking protons from the environment is the conjugated acid of that base.

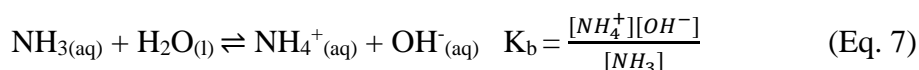


Acids or bases that completely dissociate into their ions in water are called strong acids, those that are partially ionized and those with a certain ionization constant value are called weak acids or bases. Since strong acids can give protons very easily, the conjugated bases of these acids are quite weak. In addition, strong bases are conjugated to a weak acid that cannot easily deliver protons because they attract protons strongly. Conjugated acid of strong bases is weak (Biryol, 1995).

Weak acids or weak bases that do not fully ionize in their aqueous solution are known as weak electrolytes. In solutions of these compounds, the acid or base is in equilibrium with its ionized form. For example, the following reaction equation and equilibrium expression can be written for nitrous acid ( $\text{HNO}_2$ ), which is a weak acid.



$K_a$  is the ionization constant of weak acid. To give another example, a small part of ammonia ( $\text{NH}_3$ ), which is a weak base, in aqueous solution is ionized by the following reaction.



Here  $K_b$  is the ionization constant of the weak base. Aqueous solutions containing a weak acid and its salt, or a weak base and salt, and which resist pH change by the addition of acid or base, are called buffer solutions. Consider a buffer solution consisting of the weak acid HA and its salt MA (M: methal). The ionization balance of the weak acid, the ionization equilibrium constant expression and the ionization of its salt (100% ionized) is given as follows.



$$K_a = \frac{[\text{H}_3\text{O}^+][\text{A}^-]}{[\text{HA}]} \quad (\text{Eq. 10})$$

If  $[\text{H}_3\text{O}^+]$  is taken from the expression of the ionization equilibrium constant, equation below is obtained.

$$[\text{H}_3\text{O}^+] = K_a \times \frac{[\text{HA}]}{[\text{A}^-]} \quad (\text{Eq. 11})$$

If the minus logarithm is taken on both sides of the equality as given below equation,

$$-\log[\text{H}_3\text{O}^+] = -\log K_a - \log \frac{[\text{HA}]}{[\text{A}^-]} \quad (\text{Eq. 12})$$

$$\text{pH} = \text{p}K_a - \log \frac{[\text{HA}]}{[\text{A}^-]} = \text{p}K_a + \log \frac{[\text{A}^-]}{[\text{HA}]} \quad (\text{Eq. 13})$$

Equation 13 is obtained. The same equation can be written as below.

$$\text{pH} = \text{p}K_a + \log \frac{[\text{Base}]}{[\text{Acid}]} \quad (\text{Eq. 14})$$

This equation is known as the Henderson-Hasselbalch equation and is commonly used for buffer solutions (Özcan, 2011)

Dissociation constants are obtained by several methods those are potentiometry, UV–VIS spectrometry, liquid chromatography (Dempsey et al.), capillary electrophoresis (CE), fluorometry, polarometry, voltametry, calorimetry, kinetic method, solubility, partition and NMR. Potentiometric and UV/VIS

spectrometry methods are the most commonly used methods for  $pK_a$  determination due to their simplicity, reproducibility and accuracy (Babić et al., 2007; Reijenga et al., 2013).

The determination of ionization constants by spectroscopic method is more time consuming. However, if the solubility of a substance is too low to be determined by the potentiometric method or the  $pK_a$  value of the substance is less than 1.5 or greater than 11, the spectroscopic method is the most ideal in such cases.

Absorption is mostly caused by the excitation of bonding electrons in molecules. Consequently, it is used in the identification of functional groups in a molecule by molecular absorption spectroscopy and also in the quantitative determination of compounds including functional groups. Spectrophotometers, used in UV/Vis region, are divided into two that single beam spectrophotometers and double beam spectrophotometers.

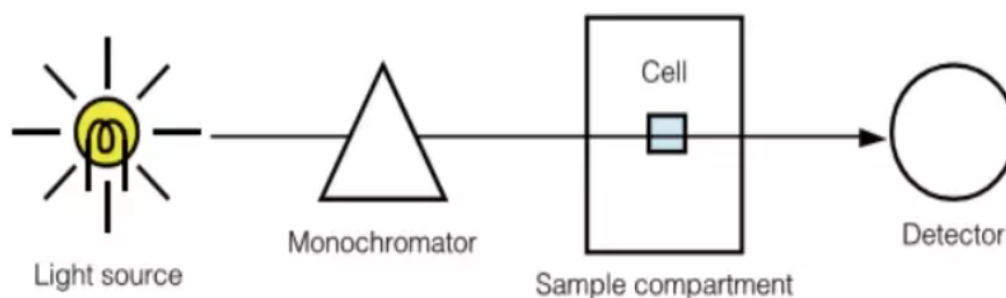
### ***Single Beam Spectrophotometers***

In the single spectrophotometers, beam path is closed against the solvent of the same wavelength, zero transmittance adjustment and 100% transmission adjustment is made by opening the beam path. Or, in computer-controlled instruments, the spectrum of the solvent is taken and subtracted from the spectrum of the analyte, preventing interference from absorbance of the solvent.

In single beam spectrophotometers, the components are all placed in the same light path. This instrument has three main adjustment knobs: One is the knob that enables the mechanical rotation of the optical system or prism used in the instrument. The second button is to set the galvanometer "zero" transmittance by completely covering the light path. After the wavelength at which the measurement will be made is adjusted with the first button, the light path is turned off and the "zero" setting is made with the second button. The third button changes the width of the range through which the light passes. Then, with the third button, the width of the gap where the light passes is changed and the galvanometer is brought to 100 by using only the solvent in the sample container. Zero and 100 adjustments must be made again at each wavelength.

Figure 2.

*Single Beam Schematic Diagram (World, 2021)*

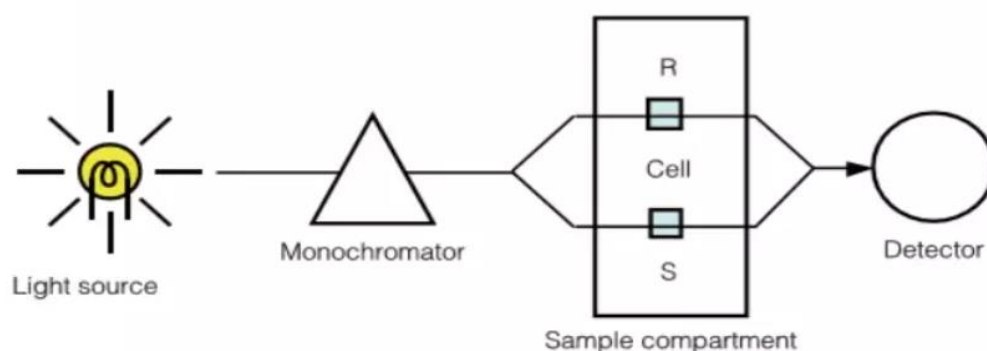


### ***Double Beam Spectrophotometers***

Instead of adjusting 0 and 100 settings separately for each wavelength in double beam devices, the mechanical chopper split the light is divided into two; these are sample beam and reference beam with same intensity. Thus, the measurement time is shortened (Nilapwar et al., 2011).

Figure 3.

*Double Beam Schematic Diagram (World, 2021)*

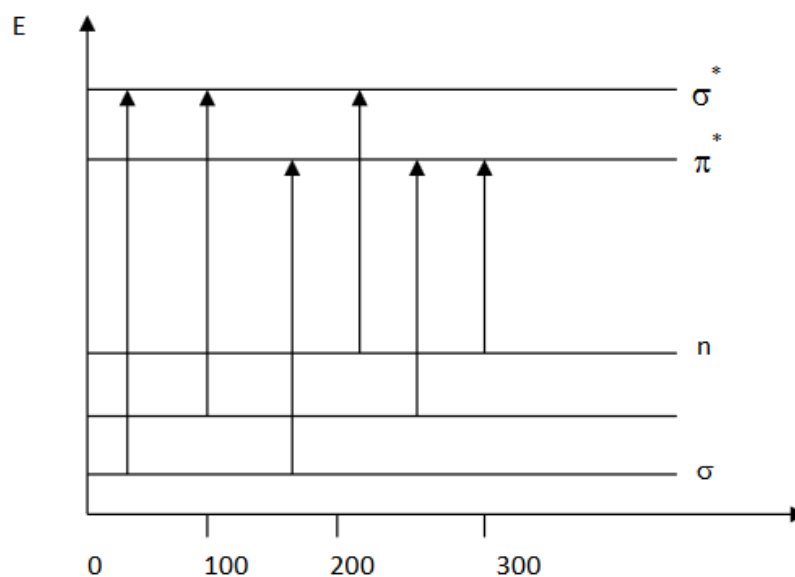


Ultraviolet light is radiation with a wavelength of 10-400 nm and is located in the electromagnetic spectrum between X-rays and the visible region. the visible region is in the 400-800 nm region of the electromagnetic spectrum. Molecular absorption spectroscopy is based on the measurement of the permeability (T) or

absorbance (A) of a solution in a cell with a beam path of light between 190-780 nm wavelengths. This absorption is mostly caused by the excitation of bonding electrons in molecules, as a result of which molecular absorption spectroscopy is used in the identification of functional groups in a molecule and also in the quantitative determination of compounds bearing functional groups.

Figure 4.

*Electronic Transitions*



$\sigma \rightarrow \sigma^*$  transitions are observed in the distant UV region as they require very high energy. In a molecule, an electron in the bond orbital is stimulated to the anti-bond orbital by absorbing a beam in the Vacuum UV region. The  $\sigma$  electrons of the C-C and C-H bonds make such transitions.

$n \rightarrow \sigma^*$  transitions observed in saturated compounds carrying hetero atoms. These transitions are observed in compounds containing un-shared electron pairs (electrons in non-bonding orbitals).

$\sigma \rightarrow \pi^*$  ve  $\pi \rightarrow \sigma^*$  transitions are very weak, therefore they can not be observed when there is a strong  $\pi \rightarrow \pi^*$  transition.

$\pi \rightarrow \pi^*$  and  $n \rightarrow \pi^*$  These are the transitions of unsaturated compounds with heteroatoms. These are the most common transitions in UV / Vis spectroscopy. Both of these transitions are observed in organic compounds containing unsaturated functional groups since they contain  $\pi^*$  orbitals. In other words, these unsaturated absorbing centers are called chromophores (Nilapwar et al., 2011). UV-VIS spectra have four kinds of transitions between quantized energy levels. The proximate wavelength ranges for these absorptions are shown in Table 1.

Table 1.

*Electronic Transition Involving n,  $\sigma$  and  $\pi$  Molecular Orbitals (Nilapwar et al., 2011).*

Transition	Wavelength Range (nm)	Examples
$\sigma \longrightarrow \sigma^*$	< 200	C–C, C–H
$n \longrightarrow \sigma^*$	160 – 260	H <sub>2</sub> O, CH <sub>3</sub> OH, CH <sub>3</sub> Cl
$\pi \longrightarrow \pi^*$	200 – 500	C=C, C=O, C=N, C=C
$n \longrightarrow \pi^*$	250 – 600	C=O, C=N, N=N, N=O

Solvent, temperature and molecular structure are factors affecting electronic transitions. The main variables affecting the absorption spectrum of a substance are the type of solvent, the pH of the solution, the temperature, the electrolyte concentration and the presence of degrading substances.

Continuous light sources such as D<sub>2</sub>, H<sub>2</sub>, W, Xe, mercury vapor lamp are used in the UV-visible area. Tungsten filament lamp emits light in the visible and near IR region (320-3000 nm). If there is some iodine or bromine vapor in the tungsten lamp, the life of the lamp increases and this lamp is called tungsten-halogen lamp. Most commonly used lamps in the ultraviolet region are hydrogen and deuterium electrical discharge lamps. These lamps emit light between 180-380 nm. D<sub>2</sub> lamp, which is more expensive and longer lasting, has a much higher light intensity than the H<sub>2</sub> lamp. Xe arc lamp is a strong and continuous light source that can be used in the entire UV-visible region (190-700 nm). Mercury vapor lamp is a light source that can



radiate in both areas. The mechanisms that produce monochromatic light in a single wavelength from the polychromatic light coming from the light source are called monochromators. Prism or optical mesh is used as a monochromator in UV / Vis. As a detector, photomultiplier tube or photovoltaic tube is used.

Good-quality absorption cells that are compatible with each other must be used for accurate spectrophotometric analysis. Cuvette material should not absorb at the measurement wavelength. Glass and quartz materials are mostly preferred in cells. In addition to the measurement wavelength, glass and quartz have extremely good chemical resistance, except for use with strong alkaline solutions. It should not be touched by hand and the paper used for lens cleaning should be used to wipe, and the use of tissue paper should be avoided. After the cells are used, rinsing with water and ethanol is sufficient for cleaning cells with scratched surfaces should not be used. In summary, the cuvette type (material) is selected according to the measurement wavelength and the solvent used.

### **Polarography**

The method in which mercury is used as the working electrode is called polarography, and the response curve obtained is called polarogram. It is a three-electrode system. In this method, a voltage scan that varies linearly with time (mercury) is applied to the working electrode (mercury) and the current response of the analyte is examined. Many reduction reactions can be studied at this electrode, due to the large overvoltage of the hydrogen gas on it. On the other hand, since the oxidation of mercury is easy, it cannot be operated at positive voltages more than +0.40 V (SCE) with this electrode. It is a very suitable method for qualitative and quantitative analysis. Polarography was first discovered by Jaroslav Heyrovsky in 1922 (Heyrovský & Zuman, 2013) .

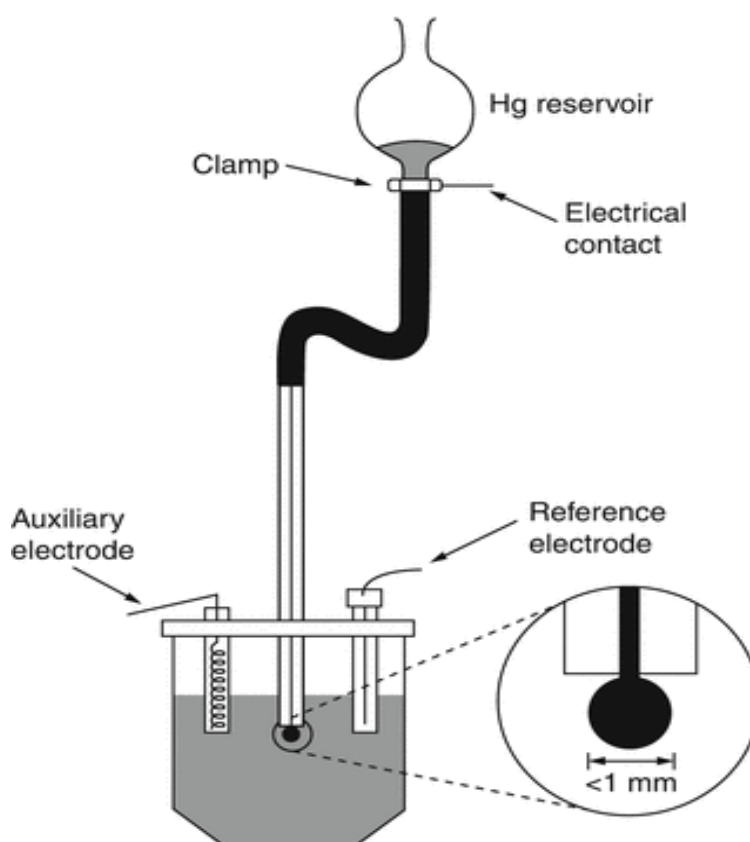
A polarographic cell contains a small easily polarized microelectrode, a large non-polarized electrode, and the solution to be analyzed. The microelectrode where the analytical reaction takes place is a mercury surface in the area of a few mm.; the mercury flows by its own weight continuously from a very thin capillary in equal drops (Lee & Hu, 2014) .With the dropping mercury electrode used in this technique, instantly repeatable average currents can be obtained at any potential. Since a new

electrode surface is formed with each drop in DME, the behavior of the electrode is independent from the previous working.

The reference electrode in a polarographic cell is heavier and larger than the micro electrode, its behavior does not change in the passage of small currents, and remains unpolarized during analysis. For this purpose, mostly a saturated calomel electrode and salt bridge can be used. A large pool of mercury or a silver / silver chloride electrode are also widely used reference electrodes. The microelectrode is connected to the negative end of the energy source; thus, the sign of the applied potential becomes negative. If this electrode acts as a cathode, the current is also positive (Lee & Hu, 2014; Zuman, 2001).

Figure 5.

*Classical Design of The Dropping Mercury Electrode* (Lee & Hu, 2014)



### *Types of Currents in Polarography*

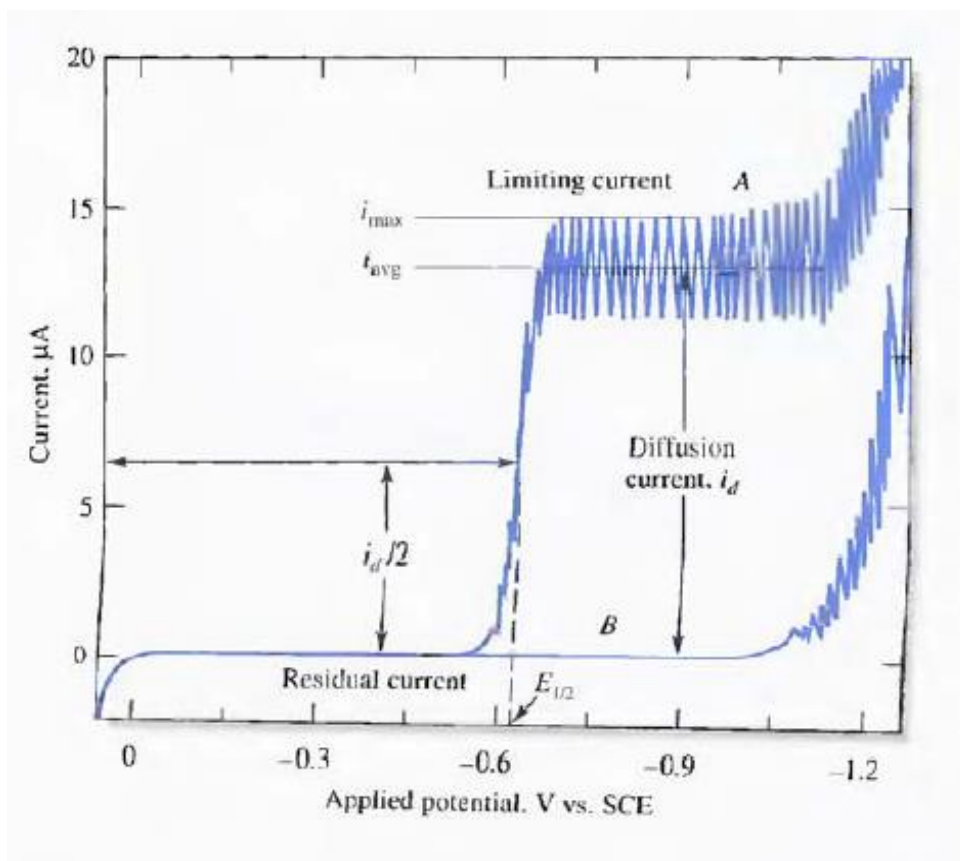
As it is seen in figure 6 there are two polarograms, one polarogram which is lower curve (B) corresponds to a 1 M of hydrochloric (HCl) solution, and the other one upper curve (B) to a mixture of 1 M HCl in  $5 \times 10^{-4}$  M cadmium ion ( $\text{Cd}^{+2}$ ) solution. A stepped current-voltage curve A is called a "polarographic wave" and this is a result of the following reaction.



$\text{Cd}(\text{Hg})$  indicates elemental cadmium dissolved in mercury. The sharp rise in current seen in both curves around -1V is due to the reduction ions of hydrogen ( $\text{H}^{+}$ ) to occur hydrogen. B polarographic wave is formed in the presence of the "support electrolyte". In the example given above, hydrogen chloride is used as support electrolyte. The polarogram given by the support electrolyte alone shows that a small current "residual current" flows through the cell even though there are no cadmium ions in the environment. A characteristic feature of a polarographic wave is the region in which the current becomes independent of the applied potential after suddenly rising; this constant current is called "limiting current". The reason for the limiting current is the restriction of the rate at which the reactant is transported to the microelectrode surface. By specially controlling the experimental conditions, the rate of transport at each point on the wave can be determined from the diffusion rate of the substance. A diffusion-controlled limited current is called "diffusion current" and is represented by the symbol  $i_d$ . The diffusion current is directly proportional to the concentration of the analyte and is therefore the most important data in the analysis. As seen in Figure 6, diffusion current is the difference between limiting current and residual current (Skoog et al., 2013).

Figure 6.

Polarograms for A, a 1 M solution of HCl that is  $5 \times 10^{-4}$  in  $\text{Cd}^{+2}$  and B, a 1M solution of HCl (Skoog et al., 2013).



Another important data is the "half wave potential" value where the current is equal to half the diffusion current that also shown in figure 6. Half wave potential is indicated by the symbol  $E_{1/2}$ . Polarograms allow us to perform both qualitative and quantitative analysis. There is a certain half-wave potential for every substance under certain conditions. This forms the basis for using polarography in qualitative analysis. In quantitative analysis, it is benefited that the diffusion current is proportional to the concentration. This relationship is given by the Ilkovich equation (Biryol, 1995).

### ***Quantitative Analysis in Polarography***

In 1934, D. Ilkovic derived a fundamental equation in which diffusion currents obtained with a mercury drop electrode can be determined. Ilkovic equation is given (at 25 °C) in Equation 16 showed that there is equality. Where  $i_d$  is the average diffusion current (mA) over a drop's lifetime;  $n$  number of electrons transferred in the reaction of one mole of the .  $D$  is the diffusion coefficient of the reactants ( $\text{cm}^2 / \text{s}$ ),  $m$  mercury flow rate ( $\text{mg} / \text{s}$ ),  $t$  is the drop time (s), and  $C$  is the concentration of the reactant ( $\text{mmol} / \text{l}$ ). 607 is found by adding several constants together. Quantitative analysis is carried out by making use of the feature that the diffusion current is proportional to the concentration of electroactive species. This relationship is given by the Ilkovic equation:

$$i_d = 607 n D^{1/2} C m^{2/3} t^{1/6} \quad (\text{Eq. 16})$$

If the height ( $h$ ) of the column of mercury is kept constant in the polarographic experiment, the flow rate ( $m$ ) and the droplet lifetime ( $t$ ) of the mercury also remain constant. When it is done at constant temperature, the diffusion coefficient also remains constant and the Ilkovic Equation takes the following form.

$$i_d = Kc \text{ or } i_d/c \quad (\text{Eq. 17})$$

Here  $C$  is the solution concentration. This equation is a line equation, it is used in quantitative analysis. The current formed here is diffusion controlled and is called diffusion current. Kinetic current and adsorption currents can also occur. The kinetic current is formed as a result of the chemical reaction of the electroactive substance, and this substance is reduced and oxidized to form a current. The concentration of the electroactive substance is determined by the rate of the chemical reaction. In the adsorption current, the current is adsorbed on the electrode surface. The reaction rate depends on the adsorbed species (Samec, 2002).

### ***Qualitative Analysis in Polarography***

Qualitative analysis is made from the S-wave obtained when the current measured against the applied potential in polarography studies is plotted. The potential corresponding to half of the wave height (the potential corresponding to  $I_d/2$ ) is called the half-wave potential and is denoted by  $E_{1/2}$ . The half-wave potential

is usually independent of the concentration of the electroactive species. Therefore, the basis of polarographic qualitative analysis is based on the half-wave potential. According to the following equation, the potential at any point on the polarogram is subtracted from the Nernst equation;

$$E = E_{1/2} + \frac{RT}{nF} \ln \frac{I_d - I}{I} \quad (\text{Eq.18})$$

This equation, which shows the relationship between the half-wave potential and the current intensity, is called the polarographic wave equation. It is understood from equation 18 that the half-wave potential in a polarographic wave is a reference point; this value is independent of reactant concentration, but it is directly proportional to the standard potential of the half-reaction (Skoog et al., 2013).

### **Polarographic methods**

After the classical correct polarography technique, the most common techniques in practice are pulse (P), differential pulse (DP), polarographic and cyclic voltammetric (CV) techniques.

#### ***In Direct Current Polarography (DCP)***

In differential pulse polarography, a direct current potential that increases with time is applied to the polarographic cell. A constant potential is applied during the entire drop-life time. A current-voltage curve is constructed by applying a series of potential steps, each step being synchronized with the drop fall. In most instruments, however, linearly changing potential is applied, with a rate slow enough that the change of potential throughout the drop-life time is about a few millivolts. The current is measured at the end of the drop life.

#### ***Puls And Differential Puls Polarography***

Classical polarography is used in the concentration range of  $10^{-2}$ - $10^{-5}$  mole/L. Because at lower concentrations, the capacitive current (residual current) is

considerably larger than the faradic current. Pulse and differential pulse polarographic methods have been developed to overcome this drawback.

In the pulse polarography technique, a single rectangular voltage pulse is sent to the electrode in the last part of the drop life to avoid charge current changes during the first part of the drop life. After the current is measured in a very short time, the voltage changes suddenly so that the load current is less than the faradaic current at the time the current is measured. The pulse polarography technique can be applied in two different ways, pulse polarography using increasing amplitude of the voltage pulse and differential pulse polarography using a constant amplitude voltage pulse superimposed on slowly increasing voltage.

The amplitude of the applied voltage pulses increases with time, and when the change in current is plotted against the voltage change, an S-shaped curve similar to the direct current polarogram is obtained. This s-curve contains steps that represent drop life. Pulse polarography gives better results than conventional direct current polarography. In differential pulse polarography, unlike pulse polarography, the amplitude of the pulse used is constant and superimposed on a slowly increasing linearly voltage. In pulse polarography, not a continuously increasing voltage is sent to the electrode, but a single rectangular voltage pulse at the end of the drop's life. Thus, residual current changes in the first part of the drop life are prevented.

### ***Cyclic Voltammetry***

One of the common polarographic techniques, cyclic voltammetry, also known as fast linear sweep voltammetry, is a versatile and useful technique and an ideal method for examining the mechanism of redox reactions. In cyclic voltammetry, a potential in the form of a triangular wave is applied to the electrode. It is used to determine the redox behavior of compounds, to explain reaction kinetics and competitor reactions.

### **Undesired conditions in polarography**

#### ***Polarogram of Oxygen***

Due to the presence of oxygen in the solution in equilibrium with air, oxygen gives a very distinct polarogram. Because this dissolved oxygen is easily reduced in the mercury drop electrode. Other analytes are hampered by the fact that oxygen

generates a wide range of polarographic waves. For this reason, inert gas is passed through the environment to remove oxygen from solutions.

### ***Polarographic Maxima***

An ideal polarographic wave is an S-shaped curve. However, most often this S-shaped curve shows a maximum at the beginning of the limiting current. An ideal polarographic wave is a curve in the form of an S curve. However, this curve often shows a maximum at the beginning of the limit current. This makes it difficult to determine the limit current. It is suggested that there are two reasons for these maximums. First, it is based on the adsorbing of reducing ions by the mercury drop. Thus, the concentration in the drop increases and hence a greater diffusion current is generated. Secondly, it is based on the rapid movement of the solution around the mercury drop. This increases the concentration at the electrode surface. Small amounts of surfactants are added to the medium to get rid of the polarographic maximum. These are methyl red, naphthol, gelatin, fuchsin etc. The adsorbents adsorb on the mercury drop surface and prevent or delay the movement of the solution to the electrode surface.

### ***Residual current***

To increase the sensitivity of the method, the residual current must be minimized. The supporting electrolyte and mercury are purified as much as possible, thus reducing the residual current and dissolved oxygen in the solution is thoroughly removed (Keser, 1996; Yılmaz, 1995)

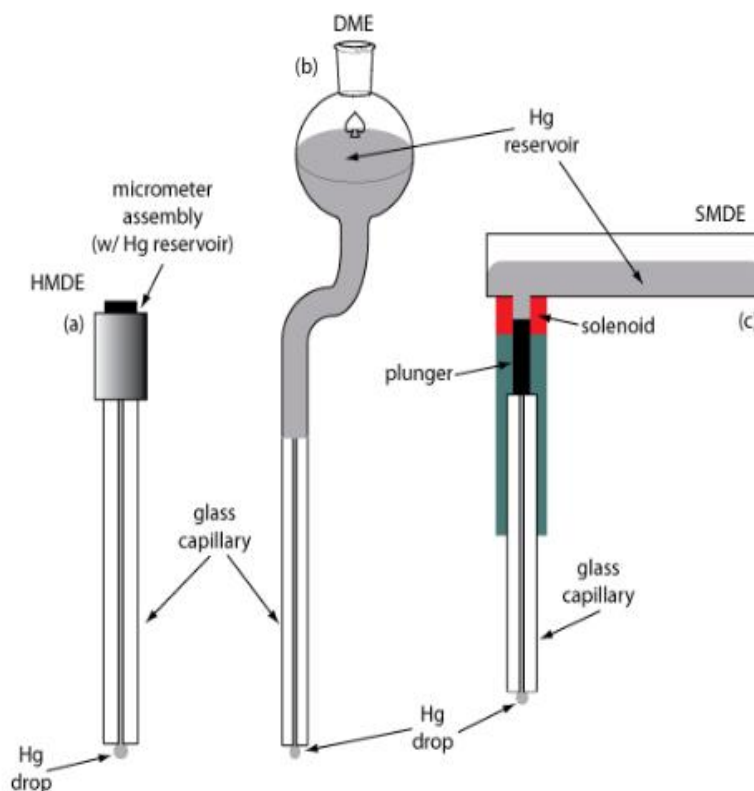
### **Types of Mercury Electrodes Used in Polarography**

In polarography, mercury is used as a working electrode, because mercury is a liquid metal and thus the electrode can be renewed after each droplet. The working electrode is often a drop suspended from the end of a capillary tube. There are three types of electrodes seen in figure 7.



Figure 7.

*Types of Electrodes used in Polarography (a) Hanging Mercury Drop Electrode (b) Dropping Mercury Electrode (c) Static Mercury Drop Electrode (Harvey, 2013b)*



### ***Dropping Mercury Electrode (DME)***

Mercury drop occurs at the end of the capillary by the effect of gravity. Drop it is constantly growing and flows from the receptacle and has a restricted life of a few seconds. After the drop falls from the capillary, a new mercury drop is formed.

### ***Static Mercury Drop Electrode (SMDE)***

This electrode contains a solenoid plunger to control the flow of Hg. Working principle of the solenoid momentarily lifts the piston, allowing Hg to flow through the capillaries and form a single suspended Hg-drop.

### ***Hanging Mercury Drop Electrode (HDME)***

The mercury drop is removed by turning a micrometer screw that pushes the mercury from a reservoir through a capillary (Harvey, 2013b) .

The first purpose of this study is to identify the theoretical  $pK_a$  and experimental  $pK_a$  values of newly synthesized coumarin derivatives by using UV-VIS spectrophotometric and potentiometric titration methods, and compare the experimental and theoretical  $pK_a$  values. Recently, theoretical support of experimental data is found useful because with the theoretical calculation methods used today, many properties of molecules can be calculated without the need of experimentation. In this way, the reliability of experimental findings increases or the chosen experimental method is supported. On the other hand, acidity constant is a very important parameter to understand the relationship between chemical properties and pharmacological effects of compounds. Therefore, the link between  $pK_a$  value and the chemical structure of the compound might be used to explain the bio-pharmaceutical properties of these substances as a part of the search in developing new synthesis methods for new drug development. On the other hand, acidity constant ( $pK_a$ ) value is an important parameter for a compound bearing an acidic group, a basic group, or both; hence, knowing it leads to understanding the differences in physicochemical properties of the ionized and neutral forms of a species. The most important impact of determining the  $pK_a$  value of a compound on the development of a new drug is in understanding its solubility. The relationship between the acidity constant and analgesic/anti-inflammatory activities of the drug candidates have been shown in the literature (Buran et al., 2021).

The second purpose of this study is to elucidate electrochemical redox mechanisms of newly synthesized coumarin derivatives by using electrochemical technique. There is no study about the electrochemical reduction and oxidation mechanisms for these compounds in the literature. In order to investigation of the electrochemical behavior of coumarin derivatives, polarographic approach has been used. This work may guide researchers for their newly synthesized compounds in the future. Elucidation of redox mechanism is also important for drug metabolism. Due to different conditions for drug molecules, molecules can be oxidized and reduce; therefore, their nature can affect their biological activities.

For every analytical method, it is of importance to understand the nature of chemical and physical processes involved in the procedure used (Zuman, 2006). Only when such processes and their sequence are understood, it is possible to understand and possibly predict the influence of other components in studied matrix on analytical results. Such understanding of reaction schemes or mechanisms is of particular importance in electroanalytical procedures, which often involve a complex sequence of chemical and physical steps (Bakirhan et al., 2018; Baymak, et al., 2018; Baymak et al., 2015; Zuman, 2006). Electrochemical methods are very useful in analysis of drug active ingredient due to their simplicity, low cost and short analysis time (Bakirhan et al., 2018; Baymak et al., 2018; Baymak et al., 2015).

## CHAPTER II

### Literature Review

#### Coumarins

There are about many naturally occurring coumarin derivatives. They occur naturally in the fruit, bark, stems and leaves of many plants, including tonka bean, acacia, lavender, apricot, strawberry, cherry and cinnamon. Besides natural coumarins isolated from plants, synthetic and semi-synthetic coumarin derivatives are also available. (Murray et al., 1982). It is known that coumarin derivatives show biological activity and are mostly used in drug research (Sashidhara et al., 2007). In addition, the presence of electron-donating amino, hydroxy and methoxy groups in the 7 position of the coumarin derivatives and the presence of electron-withdrawing benzothiazole, benzoxazole and benzimidazole in the 3 position have been found to have a bathochromic effect and strong fluorescence effect (Jagtap et al., 2009).

#### Photophysical and Photochemical Properties of Coumarins

The photophysical properties of coumarin derivatives vary according to the solvent environment and the groups depending on the structure. Due to some of their properties, coumarin derivatives offer a wide field of study. These properties can be classified as non-linear optical chromophore, important laser dyestuffs, and good responsiveness to solubility dynamics studies in homogeneous solutions (Jones II & Jimenez, 2001). When energy is lost in emission events, a corresponding shift to higher wavelengths is observed in the emission spectrum, and this difference is called the Stokes' shift. Studies have been carried out to develop photophysical properties such as redshift from maximum wavelengths and increase in Stokes' shifts without any decrease in fluorescence quantum yield values of coumarin derivatives. In the study, the effects of substituents in different positions were examined. It has been observed that the presence of a substituent in the 3 position of the coumarin ring causes low quantum yield and large Stokes' shift. When 5,6-benzocoumarin derivatives were compared with 8,9-benzo coumarin derivatives, it was determined that 5,6-benzocoumarins had higher emission properties. (Murata et al., 2005). It has been found that coumarin derivatives produce strong fluorescence effects by binding

electron donor substituents at the 7-position. 7-aminocoumarin derivatives as an example can be given. Also 7-aminocoumarin as a fluorescence probe can be used. When examining the fluorescence and absorption spectra of 7-aminocoumarin, some photophysical properties were determined. It has been determined that 7-amino coumarin has a highly polar environment and this is due to the specific hydrogen bond in the structure (Kitamura et al., 2007). A significant portion of coumarin dyes are used as blue, green and red additives in organic light-emitting diodes (OLEDs). However, coumarin dyes are easily self-quenching at high concentrations due to intermolecular interactions. For this reason, it is always necessary to use appropriate concentrations to produce OLEDs with luminescence efficiency in light-emitting materials (Yu et al., 2009).

### **Biological and Physiological Activities of Coumarins**

Coumarins, which are in the organic compound class and are found in the natural structure of many plants, have been used in laboratories for perfume production since 1868 and their structure was clarified in 1820. Coumarins, natural and synthetic derivatives have a wide range of use due to their effects as spasmolytic, anticoagulant and bacteriostatic agents. However, some coumarin substances have been found to have anti-inflammatory, anticoagulant and antitumor effects (Alghool, 2010; Kulkarni et al., 2009; Mihaylov et al., 2006). In another study, it was determined that coumarin and metal complexes inhibit reproduction in bacteria such as *Bacillus cereus*, *Escherichia coli* and *Pseudomonas aeruginosa* (Rehman et al., 2005). It is known that Umbelliferon, one of the simple coumarins, has antibacterial properties and Herniarin has anti-inflammatory properties (Alghool, 2010; Refat, El-Deen, Anwer, & El-Ghol, 2009).

### **Determination of Ionization constants of Coumarins**

Ionization constants ( $pK_a$ ); It is the basic physicochemical parameter that determines the acidic and basic properties of drug active substances.

In the literature, ionization constants of three hydroxycoumarin compounds were found by spectrophotometer method. The  $pK_a$  values of hydroxycoumarins were determined by pH measurements and absorption spectra

obtained at 25<sup>0</sup>C in aqueous medium. The pK<sub>a</sub> values for 5-OH, 4-Me coumarin were 8.26 and 9.14 and 7.80 for 6-OH and 7-OH coumarin, respectively (Mattoo, 1958).

In another study, pK<sub>a</sub> analysis of coumarins was performed by fluorescence spectrophotometer in the study performed in aqueous medium. The pK<sub>a</sub> value of 7-hydroxy coumarin was 7.75 and 7-hydroxy-4-methyl coumarin was 7.84 (Moriya, 1983).

In a study with capillary electrophoresis, experiments were carried out in aqueous medium at 25<sup>0</sup>C. The pK<sub>a</sub> values of 7-hydroxy-4-methylcoumarin were found to be 7.91, 7.99 and 7.90 (Nowak et al., 2016).

### **Determination of Reduction of Coumarins**

Many drug active substances and physiological active substances in the body respond to polarographic or voltammetric methods. Since drug molecules can be reduced and oxidized according to their environment, there may be changes in their activity.

In the literature, the main structure of coumarin was analyzed by polarography (25<sup>0</sup>C with SCE). A single curve was seen in the polarogram and E<sub>1/2</sub> was found to be independent of pH. Reduction peak was not found below pH<4. The resulting maxima were removed with 1% gelatin. It was found that the reduction occurred as a result of e<sup>-</sup> transfer, and H<sup>+</sup> transfer did not occur because the half-wave potential was independent of pH. It was stated that hydrodimer occurred after electron transfer. (Harle & Lyons, 1950).

An other study in the literature, the E<sub>1/2</sub> value of 4-methyl-2H-chromen-2-one was reported as -1.64 V by polarography (Petr Zuman, 1967).

In another study, it was stated that the α-pyrone ring on the main structure of coumarin was reduced to 3,4-double bond as a result of the study with DME among various alcohol types and ratios. With the obtained spectral and mathematical calculations, it was stated that dimerization occurred with the reduction of the main structure of coumarin(Orlov & Prokopenko, 1969).

In another study, it was investigated that the reduction potentials shifted to a more negative potential than coumarin potential with the substitution of electron withdrawing groups on the main structure of coumarin, which occurred in an aprotic medium. The proposed mechanism given in the article. With the addition of a single electron to a coumarin, radical and anion forms are formed. With the protonation of these intermediate products, major 4,4'-hydrodimer and a small amount of chroman-2-one are formed as the final products (Pasciak et al., 2015).

The electrochemical mechanisms of other coumarin derivatives whose electrochemical reduction mechanisms were studied in this thesis have not been studied before.

## CHAPTER III

### Methodology

#### Ionization Constant Assignment Methods

##### *UV-VIS spectrophotometry*

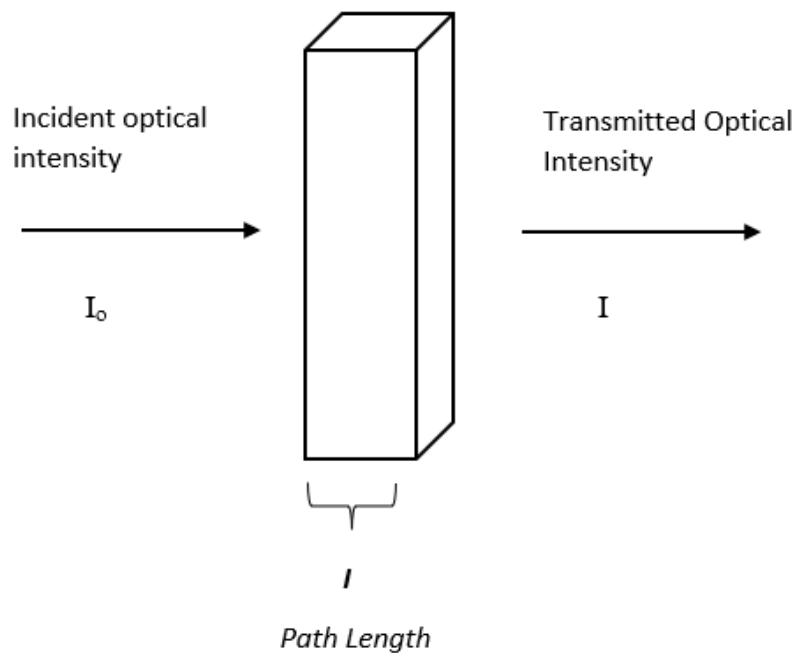
The working principle of molecular absorption spectroscopy is based on the measurement of the transmittance (T) or absorbance (A) of the solution in a cell with the path of the diffusion of light between 160-780 nm wavelengths. The radiation's power leaving from the method blank is taken to be  $P_0$ . Absorbance (A) is characterized as:

$$A = -\log T = -\log \frac{P_r}{P_0} = \log \frac{P_0}{P_r} \quad (\text{Eq.19})$$

The number of photons absorbed is proportional to the number of absorbing species in the environment. Monochromatic and  $I_0$  radiation leaves the environment at the smaller I intensity.

Figure 8.

*Standard Sample Cuvette with a Path Length of 1 cm*





Lambert-Beer's law :The amount of light passing through a solution is logarithmically inversely proportional to the way the light travels in the solution and the solution and the amount of light absorbed is directly proportional (Mäntele & Deniz, 2017).

$$\text{Transmittans (T)} = P/P^0 \quad (\text{Eq.20})$$

$$\text{Absorbans} = -\log_{10}T \quad (\text{Eq.21})$$

$$\text{Absorbans (A)} = \epsilon \cdot b \cdot c \quad (\text{Eq.22})$$

$c$  → concentration of solution (mol/L)

$b$  → the length that light travels through solution. (cm)

$\epsilon$  → molar absorption coefficient (L/mol/cm)

The establishing ionization constants is depend on the principle that the species in equilibrium absorb quite different wavelengths. The absorption spectra of organic acids and bases vary depending on the pH of the environment. Assuming that HA is an organic acid; the equilibrium in the equation 23 is established in the solution.



$$K_a = [\text{H}^+] [\text{A}^-] / [\text{HA}] \quad (\text{Eq.24})$$

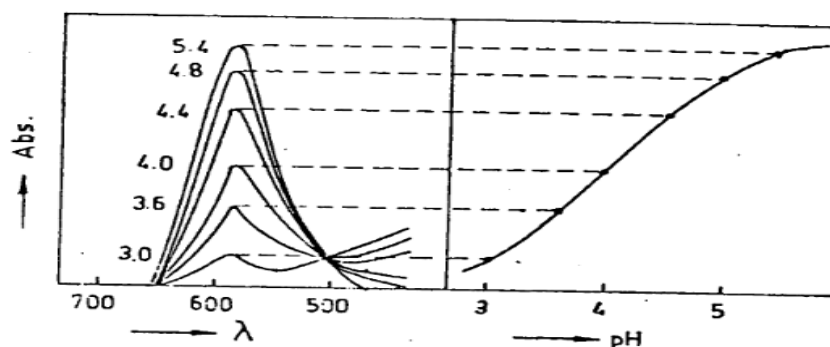
$$\text{p}K_a = \text{pH} + \log [\text{HA}] / [\text{A}^-] \quad (\text{Eq.25})$$

Equation 24 is written from this equilibrium and equation 25 is obtained by taking the negative logarithm of both sides of this equation. In the above equation, where the concentration of HA ions is equal to the concentration of A<sup>-</sup> ions, then pKa = pH. Thus the Ka value is found. For this, pH-absorption graphs of the analyzed compound are drawn with the spectra obtained depending on the pH. The pH-absorption graph drawn is given in figure 9. In the graph, HA = A<sup>-</sup> is at the midpoint of the sigmoid (s-shaped curve). To determine the midpoint, the lowest and highest absorptions of the graph must be determined. This is evident from the fact that the absorption no longer changes although the pH changes. A parallel to the pH axis is drawn from the midpoint and then a perpendicular is drawn from the point where this line intersects the sigmoid curve with the pH axis. The value shown perpendicular to

the pH axis is equal to  $pK_a$ .  $[HA] = [A^-]$  in the middle of absorption and  $\log [A^-] / [HA] = 0$  (Skoog et al., 1998).

Figure 9.

*Spectra of a Substance at Different pH Values and Plotting the pH-Absorbance Graph*



### **Potentiometric Method**

In potentiometric methods, no external current or voltage is applied. The measured quantity is the equilibrium of the system. The relationship between this equilibrium potential and analyte concentration is determined by the Nernst equation and can be used for quantitative analysis. Potentiometric methods are two-electrode systems. One of the electrodes is the reference electrode (SCE or Ag / AgCl), while the other is the working (indicator) electrodes that can change according to the purpose.

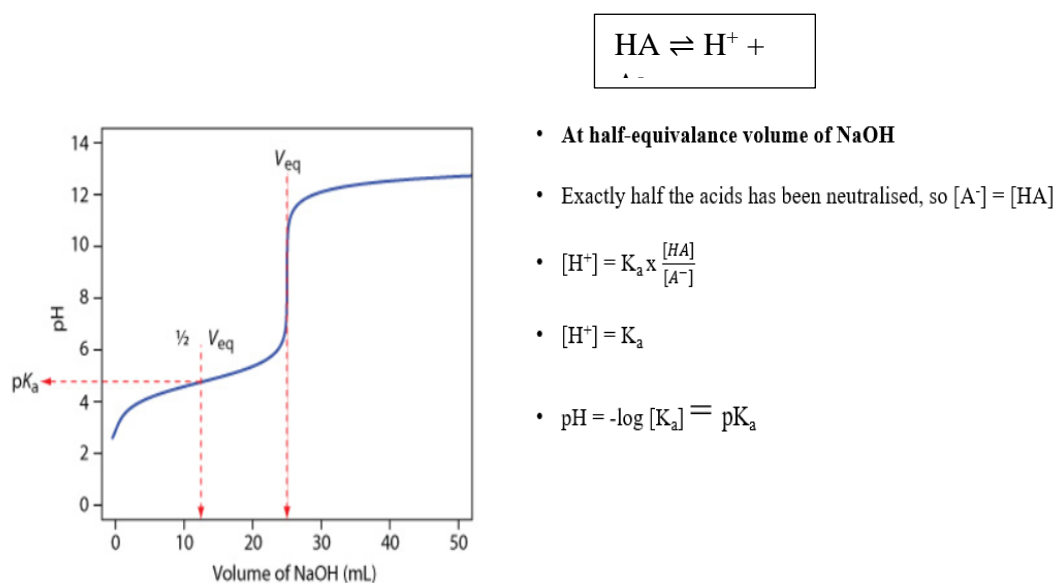
In electroanalytical applications, it is desired to know the half-cell potential of one of the electrodes, to be constant and not to be affected by the composition of the solution in the environment. A suitable electrode is called a "reference electrode". The second electrode used with the reference electrode is the "indicator electrode" and moves according to the concentration of ions or molecules in the solution.

In potentiometric titration a sample titrated with acid or base using a pH electrode to monitor the course of titration. The equivalence point of a potentiometric titration is determined by the potential of a suitable indicator electrode. In titration, cell potential (or a pH value) is measured and recorded after each addition of titrant.

At the beginning of the experiment, the titrant is added in large amounts, but as the end point is approaching, additions are made in smaller amounts. It can be understood and adjusted by the increasing potential changes after each addition of titrant. The titration curve is formed by plotting the measured pH values by adding titrant to the graph. In the S-shaped potentiometric titration curve, the equivalent point is the point where the slope of the curve is the greatest. The point where the steep drawn from half the amount of solution spent for titration intersects the pH curve gives the  $pK_a$  of the acid. It is shown in fig. below (Rıdvan Say, 2009).

Figure 10.

*Potentiometric Titration Curves* (Harvey, 2013a)



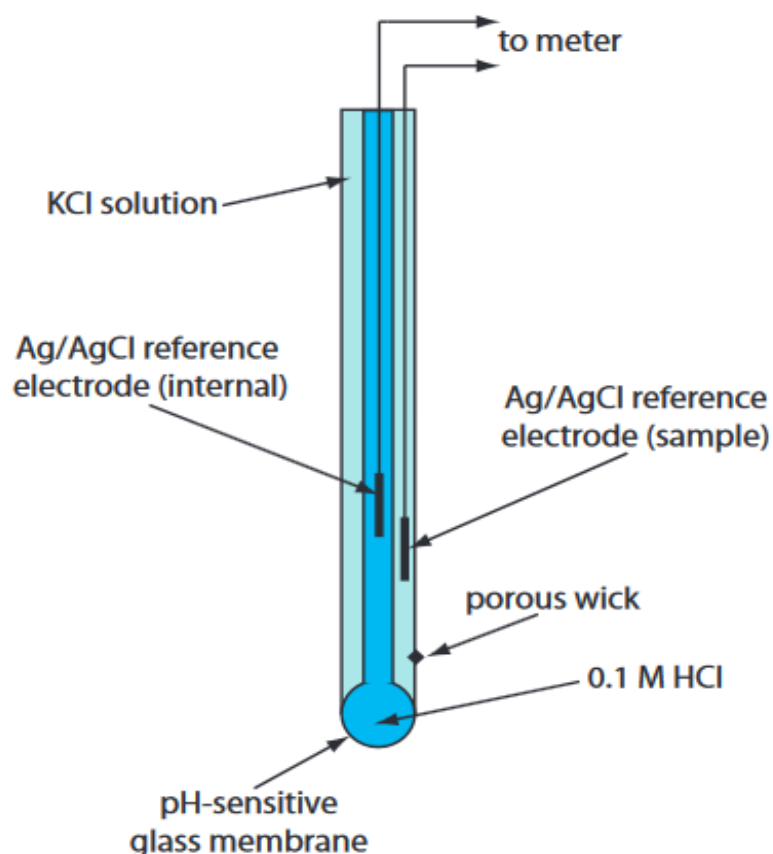
### ***Chemical and Reagents***

All chemicals used in experimental studies are of analytical purity. Sodium hydroxide, sodium acetate, sodium chloride, acetonitrile, phosphoric acid, and disodium hydrogen phosphate were purchased from Sigma-Aldrich in Germany. Ammonium chloride, sodium dihydrogen phosphate, ammonium hydroxide, hydrochloric acid, acetic acid, acetaldehyde, and methanol, were supplied by de-Haen in Germany.

Buffer solutions within the pH 1.50 to 3.50 range were prepared from phosphoric acid and sodium dihydrogen phosphate, within the pH 3.70 to 5.70 range were prepared from acetic acid and sodium acetate, within the pH 5.80 to 7.80 range were prepared from disodium hydrogen phosphate and sodium dihydrogen phosphate, within the pH 8.30 to 10.30 range were prepared from ammonia and ammonium chloride. For each buffer couples, there were five buffer solution with roughly 0.50 pH unit increments. Double distilled water was used in the preparation of the buffer solutions (Harvey, 2019).

Figure 11.

*Schematic Diagram of Glass Electrode* (Harvey, 2019)

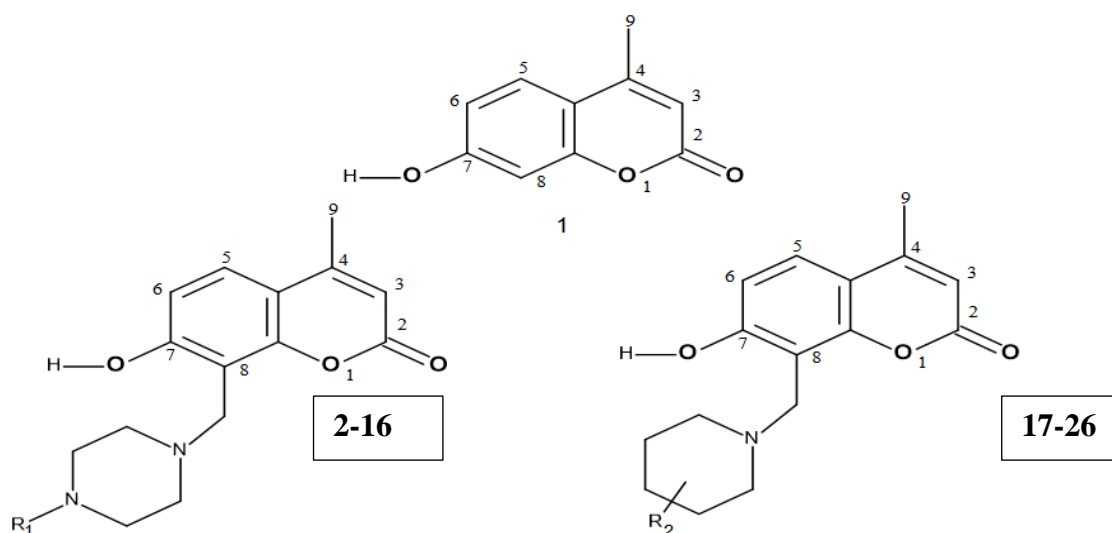


All studied organic molecules used in this work were of analytic purity and synthesized according to literature (Matos et al., 2013; Ridvan Say, 2009; Sethna & Shah, 1945). All chemical materials were used without any extra purification step.

The molecular structures of the coumarins, (2H-1-benzopyran-2-one), and their derivatives discussed in this study are given below in Table 2.

Table 2.

*List of Compounds Studied*



#	R1/R2	#	R1/R2
2	-CH <sub>3</sub>	15	<i>p</i> -NO <sub>2</sub> -Ph
3	-CH <sub>2</sub> CH <sub>3</sub>	16	<i>p</i> -OCH <sub>2</sub> -Ph
4	-CH <sub>2</sub> CH=CH <sub>2</sub>	17	H
5	-CH <sub>2</sub> CH <sub>2</sub> OH	18	4-CH <sub>3</sub>
6	-CH <sub>2</sub> CH <sub>2</sub> Ph	19	4-COOH
7	-CH <sub>2</sub> CH <sub>2</sub> CN	20	2-COOCH <sub>2</sub> CH <sub>3</sub>
8	-Ph	21	3,5-(CH <sub>3</sub> ) <sub>2</sub>
9	<i>p</i> -Cl-Ph	22	2-CH <sub>3</sub>
10	<i>p</i> -F-Ph	23	3-COOH
11	-CH <sub>2</sub> - <i>p</i> -Cl-Ph	24	3-CH <sub>2</sub> OH
12	-CH <sub>2</sub> -Naphthalene	25	-4-Ph
13	-COOCH <sub>2</sub> Ph	26	-4-OH-Ph
14	<i>p</i> -CH <sub>3</sub> -Ph		

### ***Instrumentation***

T70 UV-VIS model spectrophotometer device of PG Instruments Company was used for spectrophotometric experiments to determine the acidity constants ( $pK_a$ ). In determination of acidity constants with potentiometric method and also measuring pH values of the buffer solutions prepared, Mettler Toledo Seven Easy Model pH-meter was used. The calibration of the pH meter was carried out with standard buffer solutions of Merck HC 748513 standards (pH: 4, 7, 10). Heidolph MR 3004 magnetic stirrer and heater, Bandelin Sonorex digital ultrasonic bath were used to regulate the experimental conditions. OHAUS Analytical Plus Balance was used to weigh samples and chemicals. Eppendorf automatic pipettes were used for volumetric measurements. Polarographic Analyser Model ENTEK 2017-DME model polarography was used for reduction mechanism of compounds.

### **Methods And Calculations**

UV-VIS spectrophotometric method has been used for the determination of  $pK_a$  values of coumarin derivatives. In this spectrophotometric study, concentrations of stock solutions of all coumarin derivatives were prepared in acetonitrile at  $1 \times 10^{-3}$  M concentration. Subsequently, stock solutions of all derivatives were diluted with the selected buffer solution to achieve the final concentration of coumarin derivatives as  $3.0 - 6.0 \times 10^{-5}$  M. Prepared solutions were preserved in capped bottles to prevent the entrance of carbon dioxide. The absorbance-wavelength values, obtained after measurements of each sample, were transferred into the computer and plotted. The most suitable wavelength for all pH values was selected, and absorbance vs. pH plots were generated for a chosen wavelength. The  $pK_a$  values for each compound were determined from these spectral data obtained from three independent experiments in the wavelength range of 200 - 400 nm. The ionic strength was kept constant at 0.150 M for all solutions with sodium chloride.

In potentiometric analysis experiments, all studied aqueous solutions contained 0.5 mL of sodium chloride to keep the ionic strength at 0.150 M and coumarin samples that were dissolved in organic solvents (generally acetonitrile) at a bulk concentration of  $0.5$  to  $1.0 \times 10^{-2}$  M and were stirred at room temperature using a magnetic stirrer. Dissolution of some substances took place in dimethyl sulfoxide (DMSO), and some needed heat to dissolve. The amount of solvent used was

increased for some coumarin (7-hydroxy-4-methylcoumarin) derivatives, which did not dissolve completely in aqueous solution. Amount of solvent was adjusted up to 15% at maximum. After preparation of the solution of interest, pH was decreased to around 3 by additions of aliquots of hydrochloric acid (HCl). As a result of the titrations performed with 0.01 M sodium hydroxide (NaOH), the pH values corresponding to the volumes added were recorded and put into charts, and then  $pK_a$  values were calculated.

### ***Computational Calculations***

Coumarin derivative compounds were simulated and their  $pK_a$  values were calculated using the online available program MarwinSketch 20.13 (ChemAxon). This Java-based chemical software application was used to draw structure of molecules and estimate their physicochemical properties. This software regards empirically calculated physicochemical parameters (mainly Mulliken partial charges) that are obtained from ionization-site-specific regression equations. Intramolecular interactions, partial charges and polarizability parameters are used to identify the micro-ionization constants  $pK_a$  of monoprotic molecules. When a molecule contains more than one ionizable atom, as for the herein studied compounds (polyprotic compounds), it is significant to make a distinction between micro- and macro-acid dissociation constants. The micro-acid dissociation constant was acquired from the equilibrium concentration of the conjugated acid–base pairs, whereas, the macro-acid dissociation constant was endured from the global mass and charge conservation law (Harvey, 2019). In the theoretical calculation part of this study, this distinction between dissociation constants was achieved by using the mentioned computer program.

### **Polarography method**

Mechanistic studies to understand the reduction behavior of coumarins carried out by Polarography in which a series of simple buffer solutions were prepared with pH values varying between 1.0 and 12.0. These buffer solutions were prepared such that the concentration of either the acidic or basic component is held

constant throughout the series to eliminate the effect of varying buffer concentrations on the measured currents.

$\text{CH}_3\text{COOH}/\text{CH}_3\text{COONa}$  buffers are prepared by varying the composition of the acid component from in order to achieve supporting solutions of pH varying from 3.7 to 5.7. Similarly, ammonia buffers are prepared by using  $\text{NH}_3$  and  $\text{NH}_4\text{Cl}$  for pH 8.3 to 10.3.  $\text{HCl}$  solutions of concentrations varying from 0.01 M to 0.10 M was used to achieve acidic solutions whereas  $\text{NaOH}$  solutions of the same concentrations are used to achieve an alkaline media. Phosphate buffers was used in the remaining pH range. Solutions with pH varying from 2.0 to 3.2 by using  $\text{H}_3\text{PO}_4$  and  $\text{NaH}_2\text{PO}_4$ , pH from 5.7 to 7.7 by using  $\text{NaH}_2\text{PO}_4$  and  $\text{Na}_2\text{HPO}_4$  and pH from 10.8 to 12.0 by using  $\text{Na}_2\text{HPO}_4$  and  $\text{Na}_3\text{PO}_4$ . In addition, 0.1 M  $\text{KCl}$  was added to keep the ionic strength of the medium constant.

0.01 M stock solutions were prepared by keeping the studied substances dissolved in acetonitrile in an ultrasonic bath. Substances **25, 26, 24, 9, 10** and **15** were also heated to dissolve them. The polarograms of the buffer solutions containing approximately 1% v/v acetonitrile were recorded. Final concentrations of coumarin derivatives every day were prepared freshly as 0.2 mM in buffer and by adding approximately 1% gelatin to prevent the maxima formed. Nitrogen gas was passed into the solutions to remove oxygen from the solutions placed in the cell, current-voltage graphs were obtained. Electrochemical reduction experiments carried out in a Kalousek cell in combination with a saturated calomel reference electrode (SCE). Another parameter for polarography: Pt electrode was used for auxiliary, scan rate: 5 mV/s, potential range: from -1,0 V to -1,8 V, current range :100  $\mu\text{A}$  and reservoir height was 43 cm was optimized. Polarography was calibrated with Thallium.



## CHAPTER IV

## Findings and Discussion

## Determination of Ionization Constants

UV–VIS spectrophotometry and/or potentiometry methods were used to determine the acid dissociation constant ( $pK_a$ ) values of newly synthesized coumarin derivatives in this study. The chemical structures of the studied compounds are given in Table 2. Out of the studied compounds, Compound **1** can be considered as a backbone structure of the studied group of compounds. The  $pK_a$  value for Compound **1** was calculated by both of the chosen methods and found to be 7.91 by UV-VIS spectrophotometry and 7.95 by the potentiometric method. Also, the theoretical  $pK_a$  value for this compound was calculated and found to be 7.80. According to these results the position of the protonation is proposed to be on the hydroxyl group on the 7<sup>th</sup> position of coumarin ring.

In order to confirm validity of the chosen methods, both of these methods were also applied on Compound **2** and experimental and theoretical  $pK_a$  values were obtained. The agreement between the experimentally determined values and theoretical values were acceptable as given in the Table 3.

Table 3.

*Experimental and Theoretically Calculated  $pK_a$  Values of Compounds 1-13.*

#	UV-VIS		Potentiometric		Theoretical Data	
	$pK_{a1}$	$pK_{a2}$	$pK_{a1}$	$pK_{a2}$	$pK_{a1}$	$pK_{a2}$
<b>1</b>	$7.91 \pm 0.03$	-	$7.95 \pm 0.05$	-	7.80	-
<b>2</b>	$6.80 \pm 0.08$	$8.31 \pm 0.12$	$6.84 \pm 0.08$	$8.04 \pm 0.09$	6.74	7.99
<b>3</b>	$6.85 \pm 0.07$	$8.35 \pm 0.10$	$6.99 \pm 0.09$	$8.55 \pm 0.07$	6.80	8.13
<b>4</b>	$7.06 \pm 0.13$	$9.09 \pm 0.14$	-	-	6.66	7.98
<b>5</b>	$7.07 \pm 0.07$	$9.09 \pm 0.13$	$7.17 \pm 0.08$	$9.19 \pm 0.08$	6.70	7.91
<b>6</b>	$6.84 \pm 0.07$	$8.89 \pm 0.09$	-	-	6.81	8.13
<b>7</b>	$6.51 \pm 0.04$	$8.54 \pm 0.05$	-	-	6.54	7.76
<b>8</b>	$6.63 \pm 0.04$	$8.87 \pm 0.09$	$6.75 \pm 0.06$	$8.92 \pm 0.11$	6.60	8.33

<b>9</b>	$6.40 \pm 0.10$	$8.93 \pm 0.07$	-	-	6.60	8.24
<b>10</b>	$6.42 \pm 0.11$	$8.92 \pm 0.03$	-	-	6.60	8.21
<b>11</b>	$6.61 \pm 0.05$	$9.02 \pm 0.05$	-	-	6.59	7.88
<b>12</b>	$6.88 \pm 0.08$	$9.11 \pm 0.06$	-	-	6.75	8.02
<b>13</b>	$6.68 \pm 0.08$	-	-	-	6.36	7.34

The potentiometric titration results yield two S-shaped dependence of pH on the volume of NaOH added indicating presence of two acid-base equilibria for this compound (Figure 12). This observation led to the conclusion of a dissociation scheme as given in Figure 13 for this group of compounds in which the hydroxyl group on the main ring ( $pK_{a1}$ ) and the nitrogen of the piperazine substituent ( $pK_{a2}$ ) are involved.

Figure 12.

*Amount of Added Base (NaOH) as a Function of pH for Compound 2*

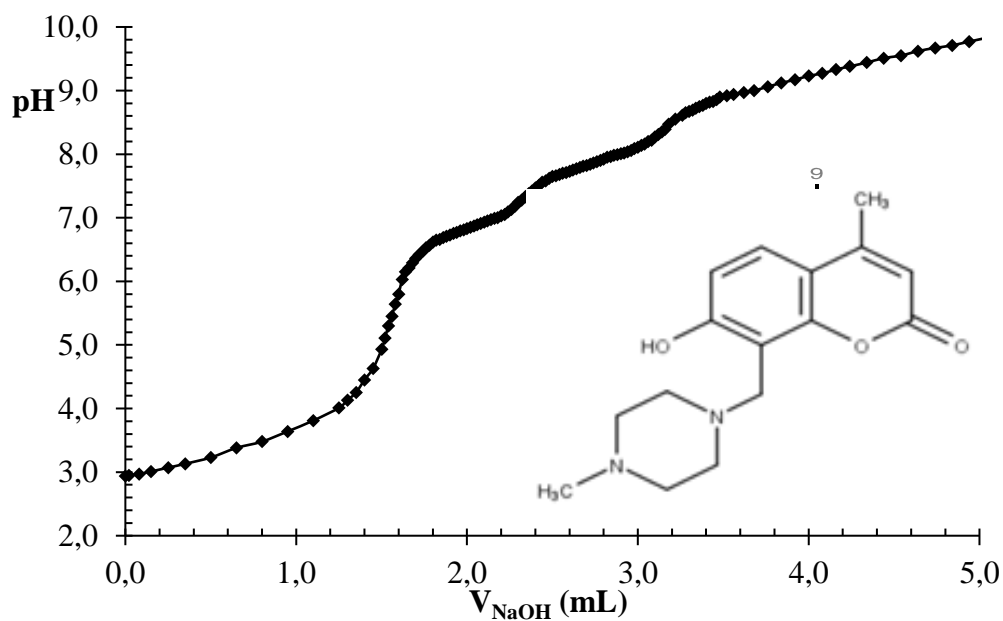
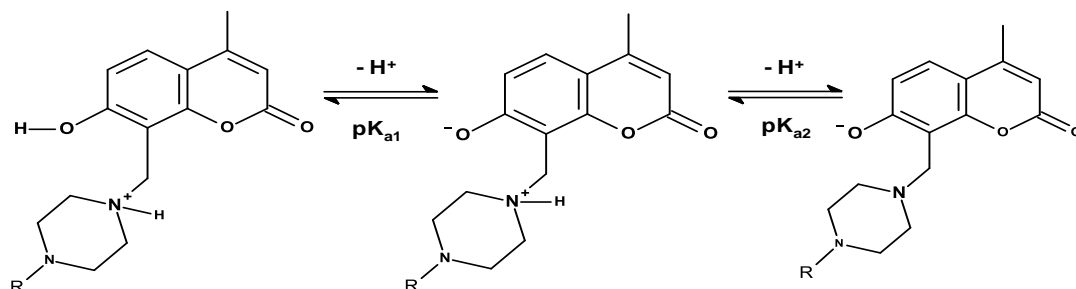


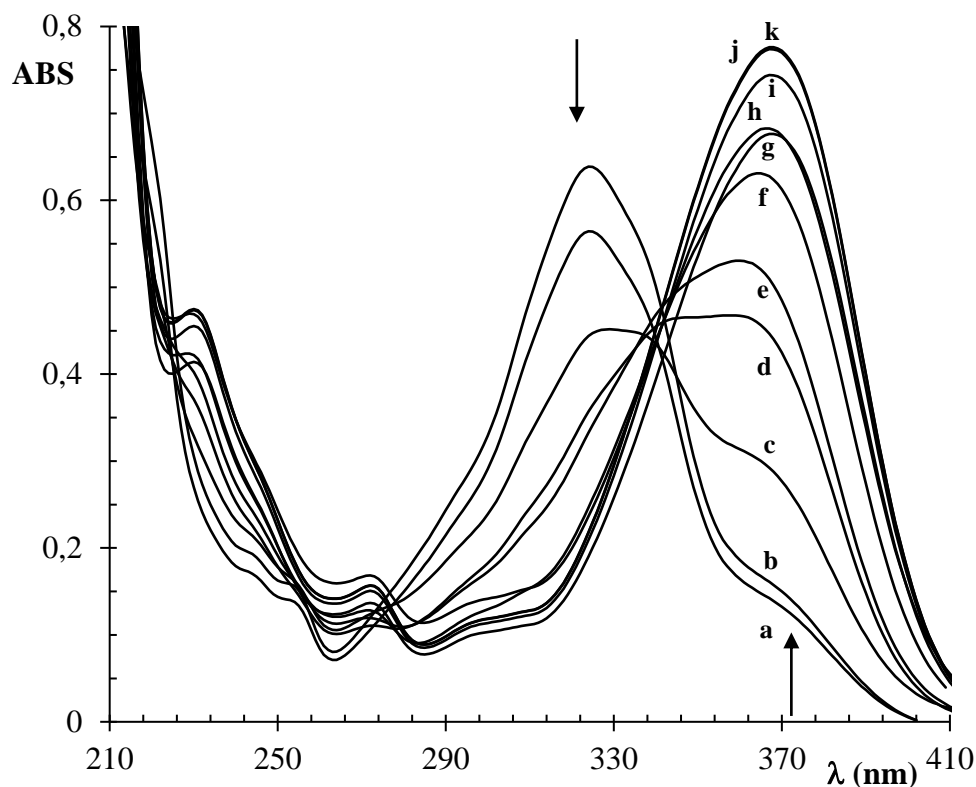
Figure 13.

*Acid-Base Equilibria of Compounds 2-16*

The UV-VIS spectra of Compound 2 in the wavelength range of 210 nm and 410 nm are given in Figure 14. Observation of an isosbestic point on the spectra at around 345 nm was also a support for the presence of acid-base equilibria. The overlapped spectra at various pH values were analyzed and  $pK_{a1}$  and  $pK_{a2}$  values were determined by plotting absorbance values against pH at three different wavelengths at which the difference between the measured absorbance values at a constant wavelength were the greatest. This procedure was repeated three times at each chosen wavelengths and reproducible values for the dissociation constants were determined at each trial. The average  $pK_a$  values for Compound 2 were reported in Table 3.

Figure 14.

*Absorbance vs Wavelength plot for  $5 \times 10^{-5}$  M Compound 2 in Various Buffered Solutions. pH Values: (a) 4.74, (b) 5.20, (c) 5.70, (d) 6.20, (e) 6.75, (f) 7.25, (g) 7.60, (h) 8.25, (i) 8.40, (j) 8.65 and (k) 8.80.*



After confirming the validity of both of the methods, Compounds **2** through **13** (compounds with piperazine substituent) were studied by UV-VIS spectrophotometry to determine their  $pK_a$  values. Even though both UV-VIS spectrophotometry and potentiometric titration methods were applied on Compound **2**, the latter method could not be applied to all the compounds due to poor solubility of them in aqueous media under the requirement of higher concentrations for the potentiometric method ( $0.5 - 1.0 \times 10^{-2}$  M in potentiometry experiments as oppose to  $3.0 - 6.0 \times 10^{-5}$  M in UV experiments). The experimentally determined  $pK_a$  values for these compounds together with theoretical calculations are given in Table 3. These sixteen compounds yield two  $pK_a$  values similar to Compound **2**. Hence, it can be concluded that there are two centers for acid-base equilibria on these compounds and they may be present in the form of zwitter ions depending on the pH of the medium. The difference between  $pK_{a1}$  and  $pK_{a2}$  values for this group of compounds is in the range of 1.5 to 2.6 pH unit. This moderate difference between the  $pK_a$  values

resulted in observation of an isosbestic point for this group of compounds in their UV-VIS spectra as a proof of presence of two equilibria.

As a result of the experiments a comparison between the two chosen experimental methods could not be achieved for this group of compounds, hence, comparison could be done only within the group and between the theoretical and experimental values. As can be seen, the agreement between experimental and theoretical  $pK_{a1}$  values for all twelve compounds is remarkable with a maximum of 0.4 pH unit difference. On the other hand, there are larger disagreement between experimental and theoretical  $pK_{a2}$  values for some of the studied compounds as well as the experimental  $pK_a$  values within the group. The compounds with higher experimental  $pK_{a2}$  values when compared to the theoretical ones were those that bear methyl moiety which acted as an electron-donating substituent to the piperazine ring making the nitrogen bonded to this substituent more basic when compared to the other group members. Compounds **17** through **26** have slightly different chemical structures, namely, the type of ring structure on the substituent group is different, bearing a single nitrogen as opposed to Compounds **2** through **16**. Out of these compounds, Compounds **17**, **20**, and **21** could not be studied by potentiometric titration method due to the solubility restrictions explained above. The experimentally found and theoretically calculated dissociation constants for these eight compounds are given in Table 4.

Table 4.

*Experimentally and Theoretically Calculated pKa Values of Compounds 17-24.*

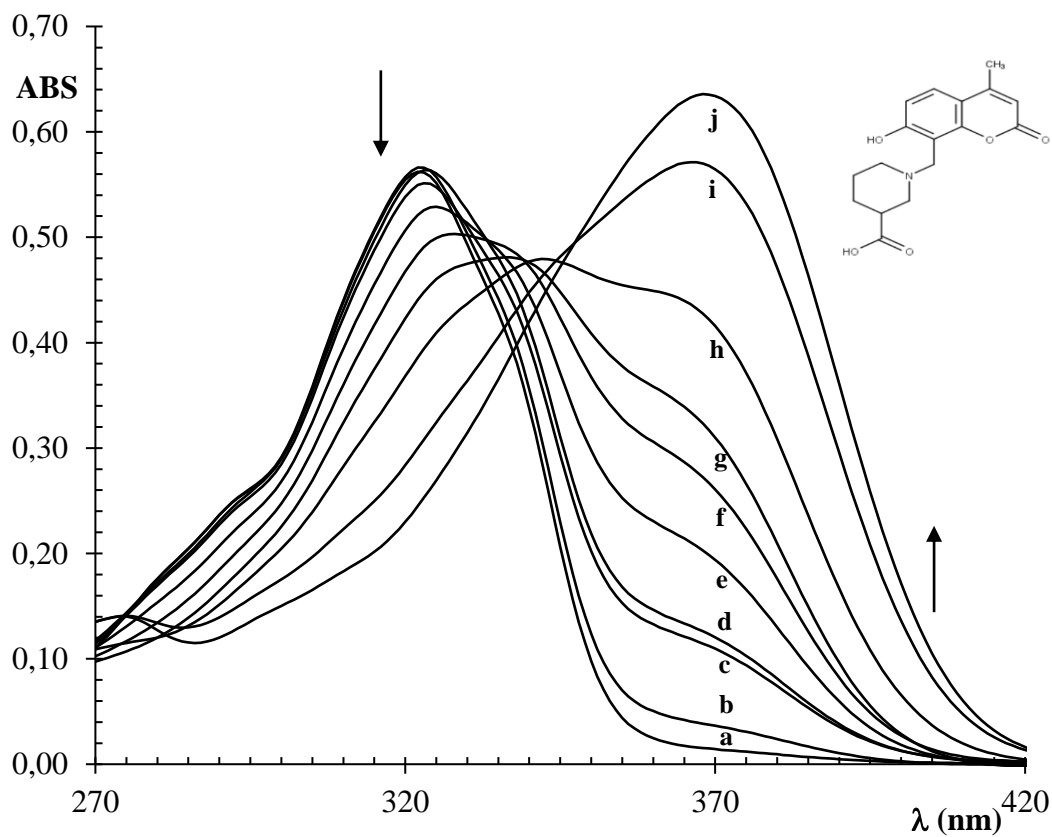
#	UV-VIS		Potentiometric		Theoretical Data	
	$pK_{a1}$	$pK_{a2}$	$pK_{a1}$	$pK_{a2}$	$pK_{a1}$	$pK_{a2}$
<b>17</b>	$6.67 \pm 0.09$	$> 8.80$	-	-	6.62	9.16
<b>18</b>	$6.69 \pm 0.10$	$> 8.80$	$6.80 \pm 0.07$	-	6.62	9.36
<b>19</b>	$6.75 \pm 0.08$	$> 8.80$	$6.78 \pm 0.11$	-	6.62	9.37
<b>20</b>	$6.33 \pm 0.04$	$< 8.80$	-	-	6.36	7.35
<b>21</b>	$6.46 \pm 0.12$	$9.58 \pm 0.11$	-	-	6.62	9.78
<b>22</b>	$6.87 \pm 0.15$	$9.28 \pm 0.05$	$6.65 \pm 0.06$	$9.30 \pm 0.04$	6.62	9.39
<b>23</b>	$6.98 \pm 0.04$	$9.97 \pm 0.08$	$7.01 \pm 0.09$	-	6.62	9.47
<b>24</b>	$6.66 \pm 0.06$	$9.65 \pm 0.08$	$6.71 \pm 0.13$	$9.78 \pm 0.08$	6.62	9.11

As can be seen in this Table 4, it was possible to calculate both  $pK_{a1}$  and  $pK_{a2}$  values for all eight compounds theoretically whereas, it was not possible to measure  $pK_{a2}$  values for compounds except **21**, and **23** by UV-VIS experiments due to the lack of observation of an isosbestic point and except for Compounds **22** and **24** by potentiometric titration due to the insufficient amount of the unprotonated form of the compound. Agreement within the experimentally found  $pK_{a1}$  values of all eight compounds as well as their similarities to theoretically calculated  $pK_{a1}$  values is remarkable.

We can compare the acidity of compounds **18** through **24** with that of Compound **17** and try to explain the unexpectedly high  $pK_{a2}$  values for this group of compounds. Compound **17** has the same main chemical structure as the other compounds in this group but with no substituent on the piperidine ring. Concerning this group of molecules, the  $pK_a$  values for the protonation of nitrogen ( $pK_{a2}$ ) were found to be close to the theoretical values and  $pK_a$  values for the deprotonation of the phenol moiety ( $pK_{a1}$ ) were found to be around 6.6. The only exception was for Compound **20**, presenting an ethyl acetate moiety of the 2<sup>nd</sup> position of the piperidine ring. For this molecule, both the theoretical and experimental values indicated a much more acidic nitrogen since the  $pK_{a2}$  values were found to drop 2 pH-units getting from an average of 9.3 for the group to 7.3. This decrease can be explained by a stabilization of the protonated nitrogen by the electron rich oxygen of the carbonyl of the ester function. The presence of an isosbestic point and separation of two protonation can be seen on the UV-VIS spectra of Compound **20** given in Figure 15.

Figure 15.

*Absorbance vs Wavelength Plot for  $5 \times 10^{-5}$  M Compound 20 in Various Buffered Solutions. pH Values: (a) 4.80, (b) 5.15, (c) 5.65, (d) 5.80, (e) 6.30, (f) 6.80, (g) 7.25, (h) 8.75, (i) 9.30, and (j) 9.90.*



A general protonation mechanism for compounds 17 through 24 is proposed in Figure 16. As an additional proof for the presence of two protonation centers for this piperidine substituted set of compounds the UV-VIS spectra of Compound 22 as a function of pH is given in Figure 17 and since this compound could also be studied by potentiometric method, its potentiometric titration curve is given in Figure 18 as well. These figures support the conclusions on the presence of two protonation centers on these molecules.

Figure 16.

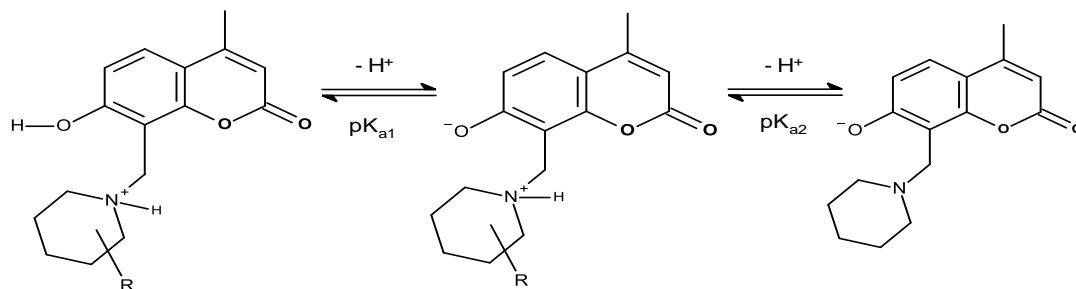
*Acid-Base Equilibria of Compounds 17-24*

Figure 17.

*Absorbance vs Wavelength Plot for  $5 \times 10^{-5}$  M Compound 22 in Various Buffered Solutions. pH Values: (a) 5.26, (b) 5.80, (c) 6.28, (d) 6.80, (e) 7.32, (f) 7.80, (g) 8.30, (h) 8.75, (i) 9.30, (j) 9.80, (k) 10.00 and (l) 10.25.*

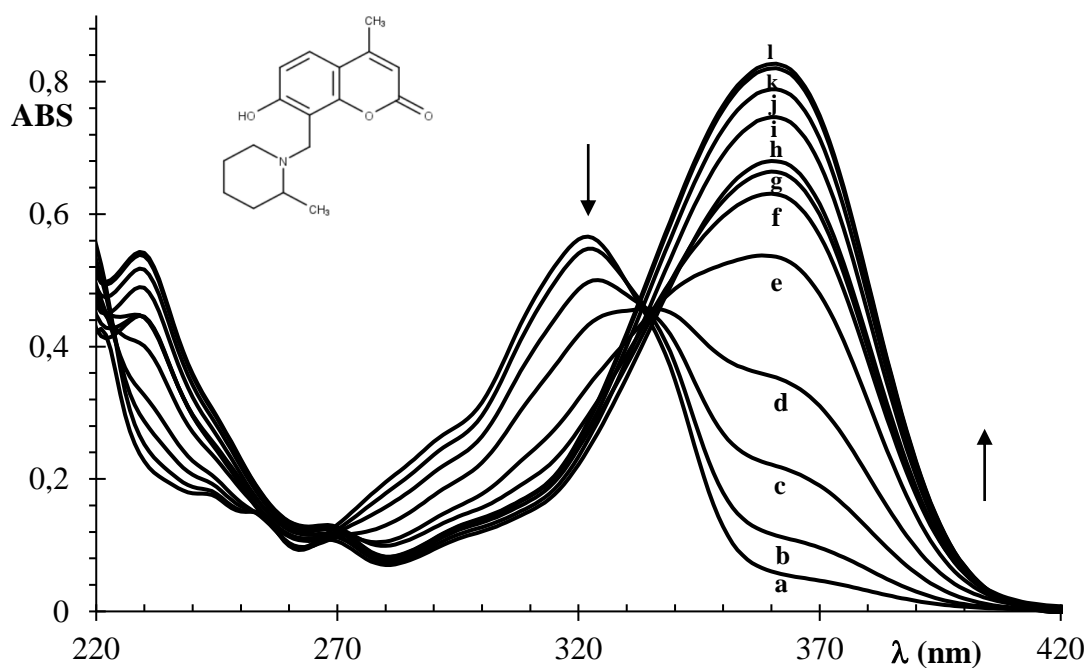
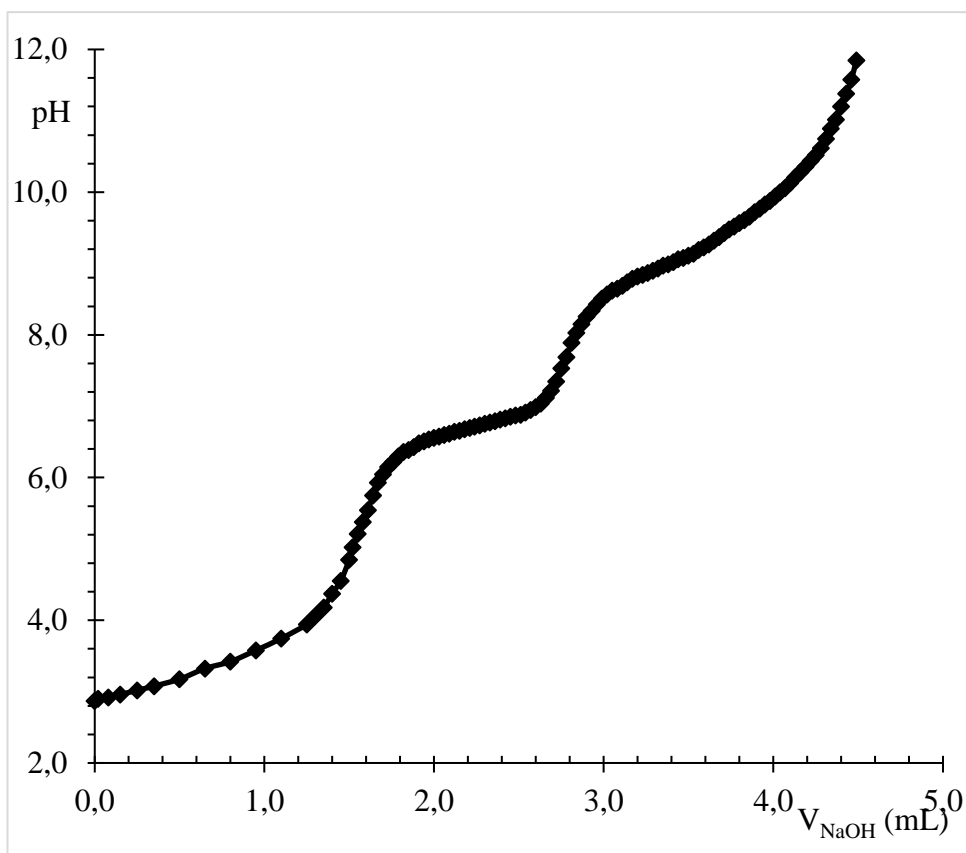




Figure 18.

*Amount of Added Base (NaOH) As a Function of pH for Compound 22.*



In order to understand the effect of chemical structure on the  $pK_a$  values in more detail theoretical calculations for some hypothetical compounds that are hydroxyl substituted on the 6<sup>th</sup> position (6-hydroxy-4-methyl-8-[(piperidin-1-yl)methyl] coumarin derivatives) were achieved. The theoretical calculation for one of these hypothetical compounds, the one that is used for comparison with Compound **17**, gave a  $pK_a$  value of 9.30 for the hydroxyl and 7.70 for the nitrogen. This approach is further applied for the other theoretical compounds and the obtained data show an increase in the  $pK_a$  of the phenolic hydroxyl of the coumarin ring when substituted at the 6<sup>th</sup> position. On the other hand, the  $pK_a$  values for the nitrogen of the heterocyclic ring for these hypothetical compounds were found lower than the values calculated theoretically for piperazine and piperidine nitrogen atoms of all studied real compounds. The comparison explained thus, indicates that the protonation of the nitrogen is stabilized for the real compounds, suggesting an effect of the oxygen atom of the hydroxyl function at the 7<sup>th</sup> position. Indeed, the proximity of the oxygen atom to the nitrogen of the heterocycle may help for stabilizing the

protonated nitrogen via an electrostatic interaction between the unprotonated negatively charged oxygen and the protonated nitrogen. The pK<sub>a</sub> values calculated theoretically for compounds with hydroxyl substituent on the 6<sup>th</sup> and 7<sup>th</sup> positions are given together for all the studied compounds in Table 5.

Table 5.

*Theoretical pK<sub>a</sub> Values for 6th Position Hydroxyl Derivatives Together with the Studied Compounds.*

#	6 <sup>th</sup> OH		7 <sup>th</sup> OH		#	6 <sup>th</sup> OH		7 <sup>th</sup> OH	
	pK <sub>a1</sub>	pK <sub>a2</sub>	pK <sub>a1</sub>	pK <sub>2</sub>		pK <sub>a1</sub>	pK <sub>a2</sub>	pK <sub>a1</sub>	pK <sub>a2</sub>
<b>2</b>	9.29	7.56	6.74	7.99	<b>12</b>	9.31	7.95	6.75	8.02
<b>3</b>	9.30	7.81	6.80	8.13	<b>13</b>	9.29	5.64	6.36	7.34
<b>4</b>	9.29	7.27	6.66	7.98	<b>17</b>	9.30	7.70	6.62	9.16
<b>5</b>	9.29	7.39	6.70	7.91	<b>18</b>	9.31	7.89	6.62	9.36
<b>6</b>	9.30	7.83	6.81	8.13	<b>19</b>	9.31	7.91	6.62	9.37
<b>7</b>	9.29	6.31	6.54	7.76	<b>20</b>	9.29	5.66	6.36	7.35
<b>8</b>	9.29	6.87	6.60	8.33	<b>21</b>	9.35	8.26	6.62	9.78
<b>9</b>	9.29	6.78	6.60	8.24	<b>22</b>	9.31	7.92	6.62	9.39
<b>10</b>	9.29	6.74	6.60	8.21	<b>23</b>	9.32	8.00	6.62	9.47
<b>11</b>	9.29	6.74	6.59	7.88	<b>24</b>	9.30	7.66	6.62	9.11

The comparison of real and hypothetical compounds explained above indicates a much more difficult protonation for the nitrogen of the compound with hydroxyl substituted on the 6<sup>th</sup> position and a more stable protonated phenol, findings thus confirming our hypothesis. Based on all the experimental evidence and the results of theoretical calculations, the positions of the protonation are proposed for both piperazine and piperidine derivatives as given in Figures 13 and 16, respectively.

In order to introduce an explanation to any existing structure-activity relationship for the studied compounds, anti-inflammatory effects of these **26** compounds together with two reference compounds given in the literature were also evaluated (Buran, 2018). In the refereed literature anti-inflammatory effects of these compounds were tested by using the nitrite inhibition assay as explained in there, and it is stated that high % Nitrile Reduction is a sign for high anti-inflammatory effect.

Under the sight of this information Compounds **11**, **12**, and **13** were concluded to have the highest anti-inflammatory activities (83%, 73% and 90% Nitrile Reduction, respectively) out of all studied compounds (Buran, 2018; Buran et al., 2021). The common functional group on the substituent for these three compounds is benzyl. The fact that the compounds with phenyl function does not show sufficient anti-inflammatory effect suggests that methylene spacer is necessary for bioactivity to reach considerable levels. Also, for these compounds, the difference between the two  $pK_a$  values has an average of about 2.3 pH units, indicating that these three compounds are among the ones with the most basic nitrogen. However, a strong emphasize on the structure-anti-inflammatory effect could not be made according to our results except proposing that aryl-substituted piperazine heterocycle substituents seem to be appropriate for the development of new anti-inflammatory drug candidates.

For all of the studied compounds with the piperazine group, two protonation centers have been proposed. On the other hand, for these compounds there are two nitrogen atoms that are prone to protonation. The protonation of the second nitrogen on the ring that bears the substituent could not be measured because the dissociation constants of two nitrogen atoms could not be distinguished.

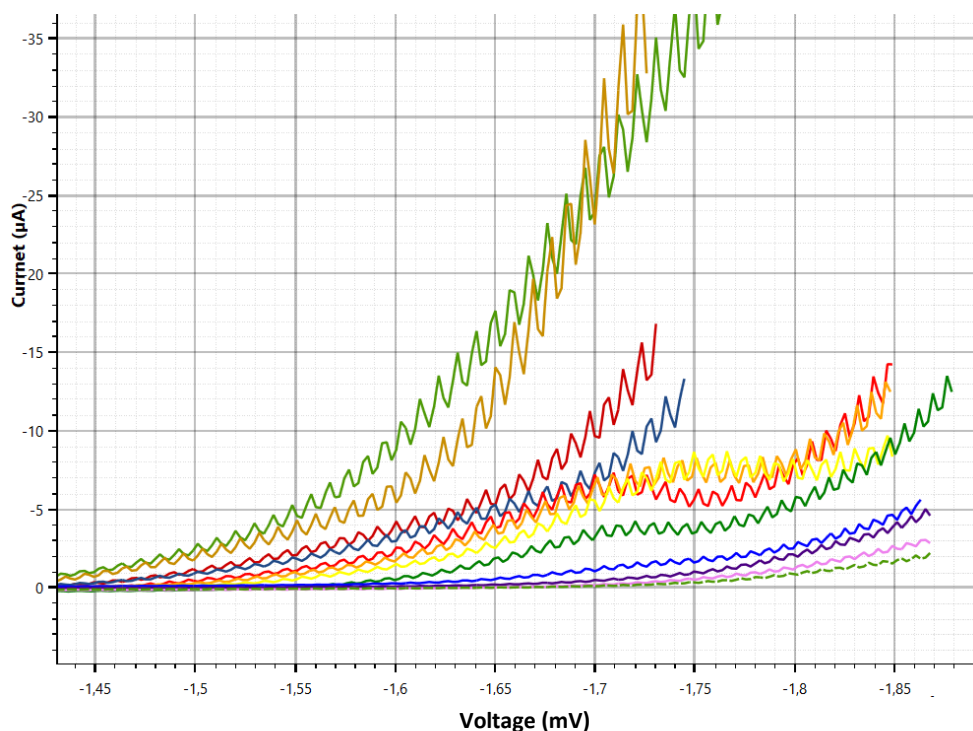
## **Polarography**

### ***Piperidine derivatives***

We continued our studies with piperidine derivatives. Initially, we started with compound **18** and studied to understand the polarographic reduction mechanism in the pH range of 3.70 to 10.25. The concentration of compound **18** was chosen as 0.2 mM at all pH values, and polarographic maxima was suppressed by addition of 1% gelatin in the electrochemical cell. No polarographic curve was found for this compound up to pH value of 6.22. After this acidity value, a peak began to be observed (Figure 19).

Figure 19.

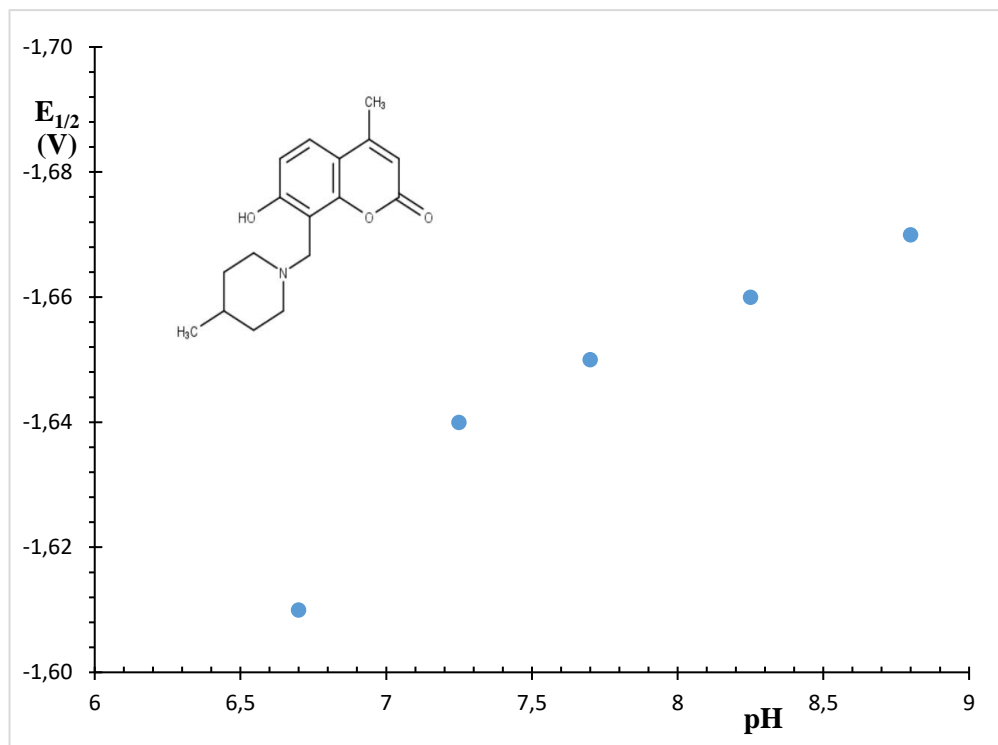
*Current-Voltage Plot of Compound 18. pH values: pH 3.85, pH 4.75, pH 5.75, pH 6.22, pH 6.70, pH 7.25, pH 7.70, pH 8.25, pH 8.80, pH 9.30, pH 9.75, pH 10.25*



It was observed that the change of *i*-*E* curves depending on acidity did not observe until pH 7.70. It has been seen that the current begins to decrease in more basic solutions. These decreases began to be observed when the pH of the solution is higher than  $pK_{a1}$  value of compound **18** (6.69). In other words, a decrease in current was observed, since the amount of its reducible form decreased when the pH is higher one pH unit than that of  $pK_{a1}$  value. At this point, it should be noted that the reducible form, which possesses negative and positive charges, is in the ionized form. It has been observed that the  $E_{1/2}$  value shifts towards a more negative value since the more energy is required for the reduction of this form. It can be seen from the  $E_{1/2}$ -pH graph (figure 20) when the hydrogen ion concentrations decrease, the reduction potential is shifted to a more negative value.

Figure 20.

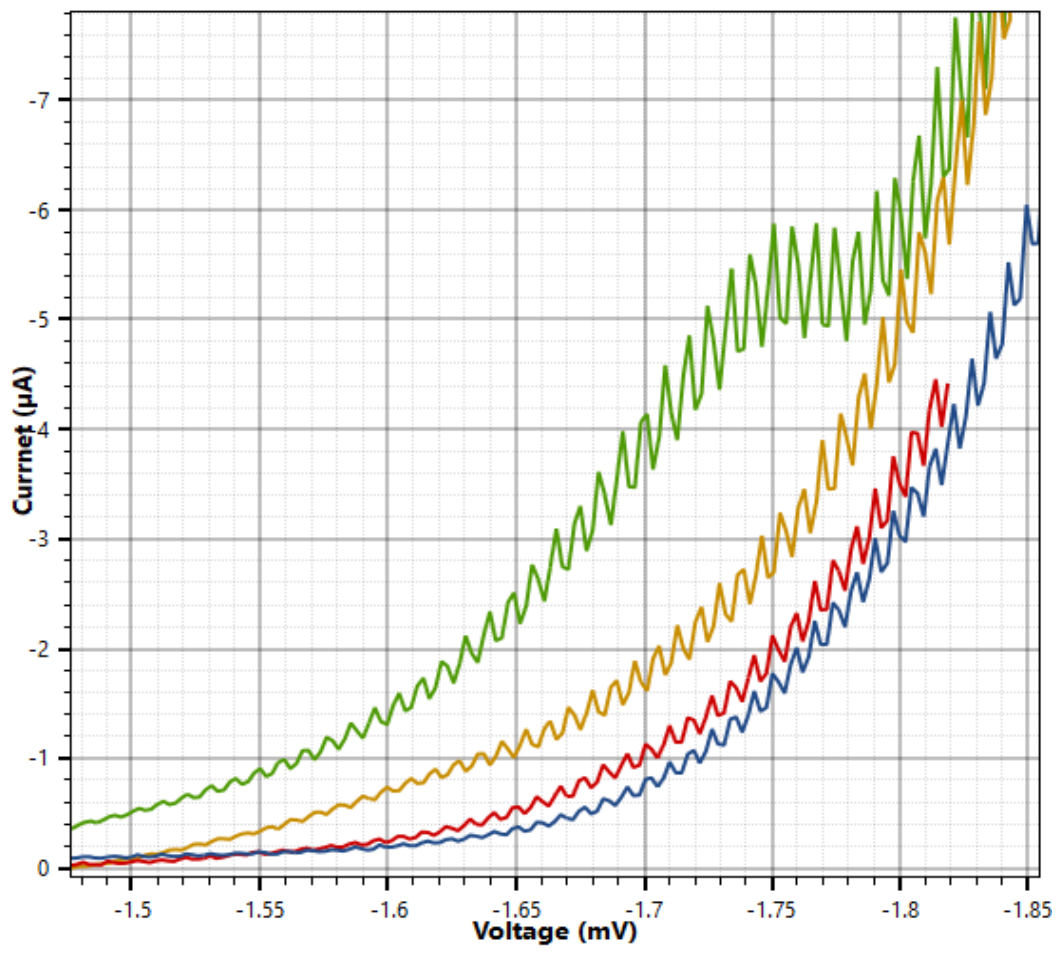
*E*<sub>1/2</sub>-pH Plot of Compound 18: pH 6.70, pH 7.25, pH 7.70, pH 8.25, pH 8.80



The second acid ionization constant value ( $pK_{a2}$ ) that was found experimentally is greater than 8.80. Therefore, when it closes to the second ionization value, the polarographic current-potential curve decreases and no peak is observed after the pH value of 9.25. This shows that the point where the reduction occurs is between two  $pK_a$  values. Therefore, the current that can be observed under reducible conditions was observed in the pH range where negative and positive charges are simultaneously present on compound **18**. Our studies were continued with the compound **25** belonging to the same group. In this substance, the piperidine ring has a phenyl group at the position of four. No peak was observed in this substance until pH 6.22, just like in compound **18**. Although a peak was observed up to pH 7.70, peak values could not be obtained due to close reduction with the supporting electrolyte solution (Figure 21).

Figure 21.

*Current-Voltage Plot of Compound 25. pH Values: pH 7.70, pH 8.25, pH 8.80, pH 9.25*



Well-developed peaks of compound **25** were observed starting from pH 7.70, and it was observed that the current value decreased with decreasing acidity. Similar to compound **18**, the peak completely disappeared after pH 9.25. It was seen that the  $E_{1/2}$ -pH dependency also changed depending on the acidity of the solution. Similar behavior was also observed for compound **26**.

Another substance from coumarin derivatives containing piperidine ring, compound **22** (containing methyl in the 2<sup>nd</sup> position in the piperidine ring), was studied at all pH values with the addition of 1% gelatin at a concentration of 0.2 mM. As can be seen from the polarograms, a curve was not seen up to pH value of 6.22. A peak began to be observed at pH 6.70 and the peak disappeared pH around 8.80. When the pH increased, a decrease in current was observed as compound **22**

increased above the  $pK_{a1}$  value ( $pK_{a1}$  6.87). That means the current decreased because the amount of the reducible form of compound decreased. Since the energy required for the reduction of the ionized form of this substance should be higher, it was observed that the  $E_{1/2}$  value shifted to a more negative value, figure (23). The reduction potential shifted to a more negative potential with a decrease in the hydrogen ion concentration in the electrochemical cell. The experimentally found  $pK_{a2}$  (9.28) value is greater than 8.80, and therefore the  $i$ - $E_{1/2}$  curve decreases when pH of medium approached to the ionization value, and no peak was observed after pH 8.80. This indicates that the observability of the reduction wave is between two  $pK_a$  values. In other words, the current that can be observed under reducible conditions can be only seen in the pH range where negative and positive charges are simultaneously present on compound **22**.

Figure 22.

Current-Voltage Plot of Compound 22. pH Values: *pH 6.70*, *pH 7.70*, *pH 8.25*, *pH 8.80*

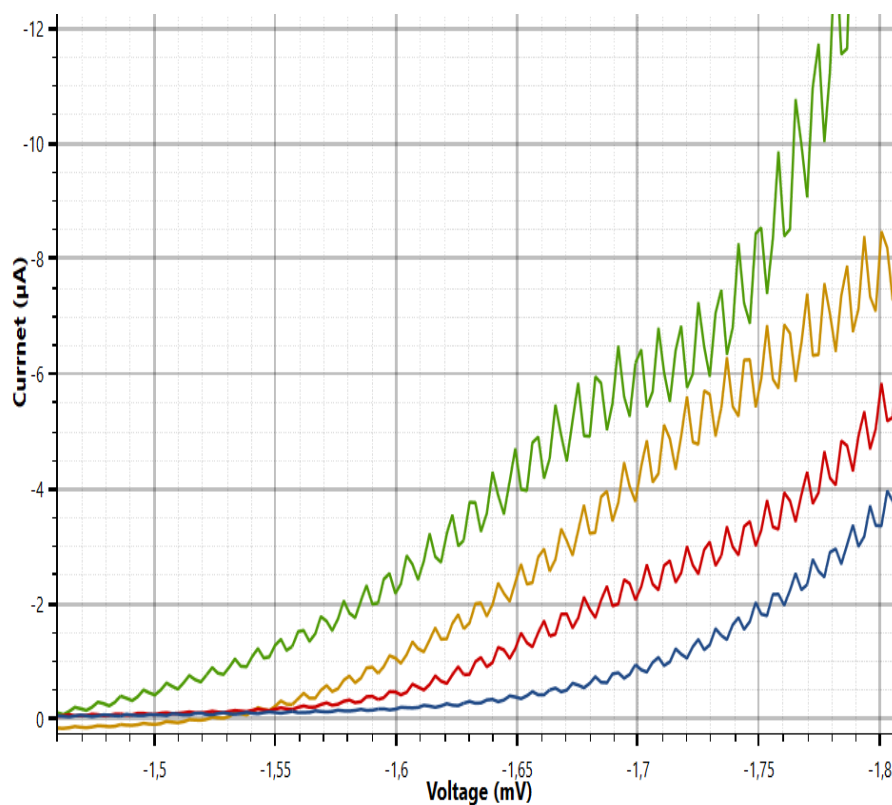
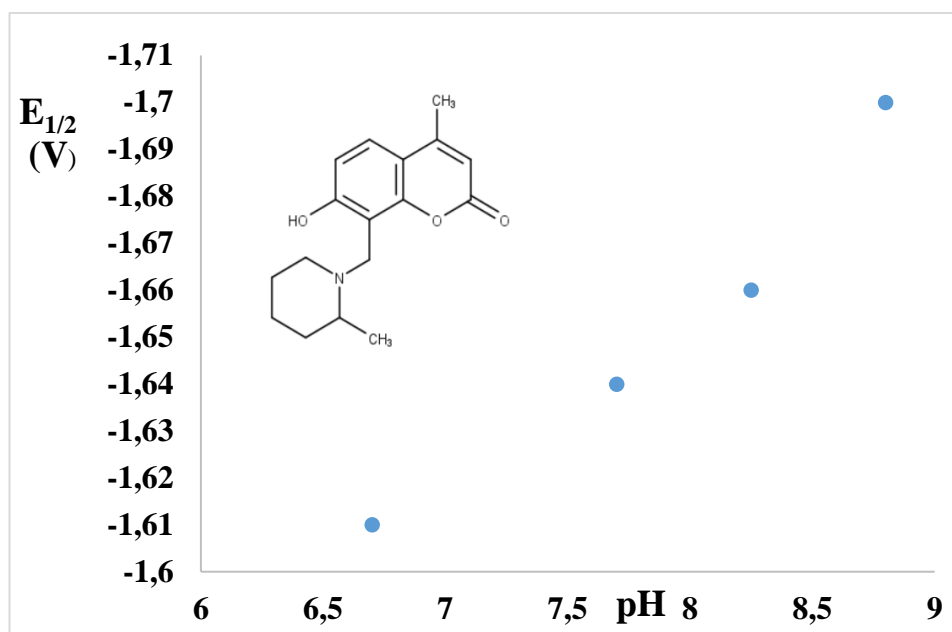


Figure 23.

$E_{1/2}$ -pH Plot of Compound 22: pH 6.70, pH 7.70, pH 8.25, pH 8.80



In the study performed with compound **17** substance belonging to the same group (no substituted group on piperidine), a peak was observed only at pHs values 7.25, 7.70, 8.25 and 8.80. According to figure 24, we can say that  $H^+$  ion transfer is dominant over  $e^-$  transfer after pH 7.70. After pH 8.80, a reduction occurs after the reduction of the supporting electrolyte.



Figure 24.

Current-Voltage Plot of Compound 17. pH Values: pH 7.25, pH 7.70, pH 8.25, pH 8.80

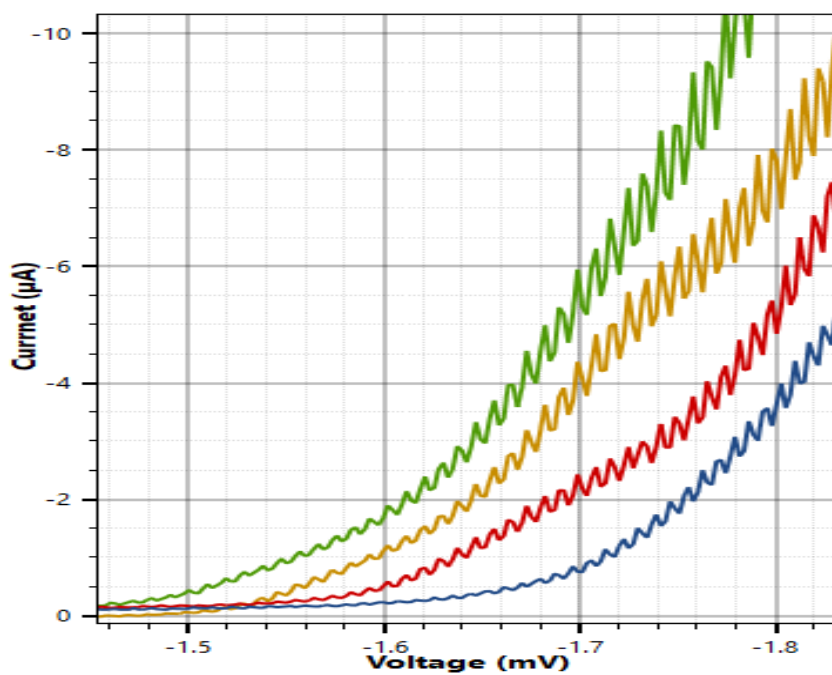
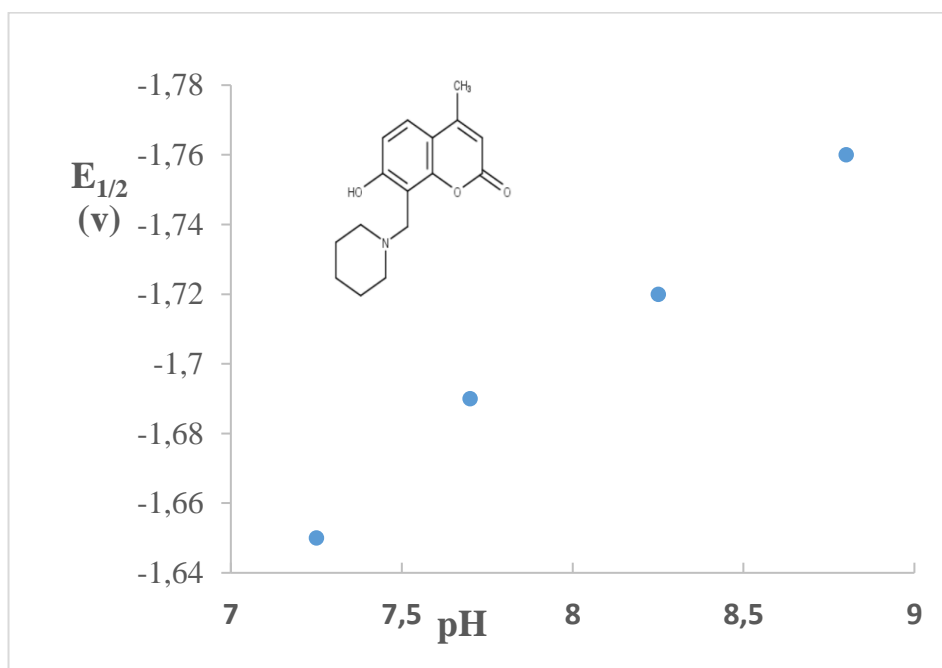


Figure 25.

$E_{1/2}$ -pH Plot of Compound 17: pH 7.25, pH 7.70, pH 8.25, pH 8.80



The current-voltage graph of the compound **24**, which was studied under the same experimental conditions and has  $-\text{CH}_2\text{OH}$  group at three positions of the piperidine ring, is given in figure 27. As can be seen in other substances, the half-wave potential shifted to more negative at increasing pH values, is given in figure 26.

No reduction waves were observed for compound **20** containing 2- $\text{COOCH}_2\text{CH}_3$  group on the piperidine ring in all pHs values studied.

Figure 26.

*Current-Voltage Plot of Compound 24. pH Values: pH 6.70, pH 7.25, pH 7.70, pH 8.25, pH 8.80*

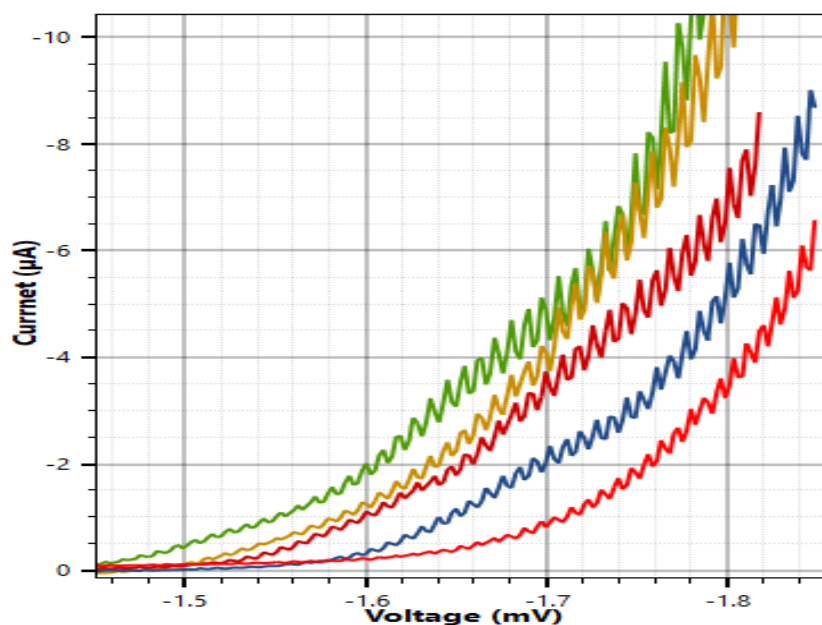
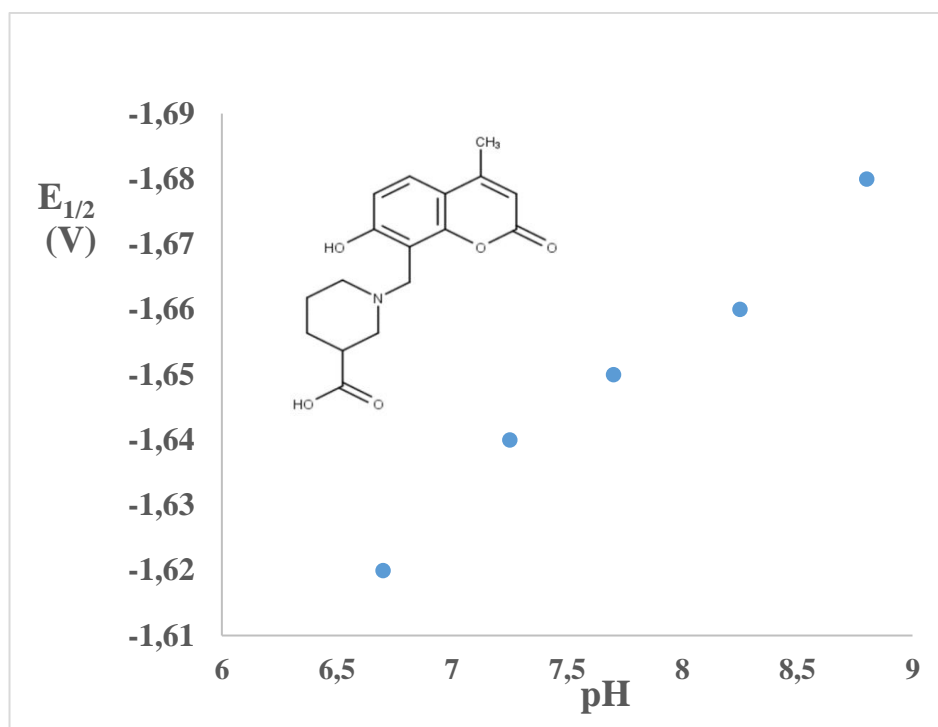


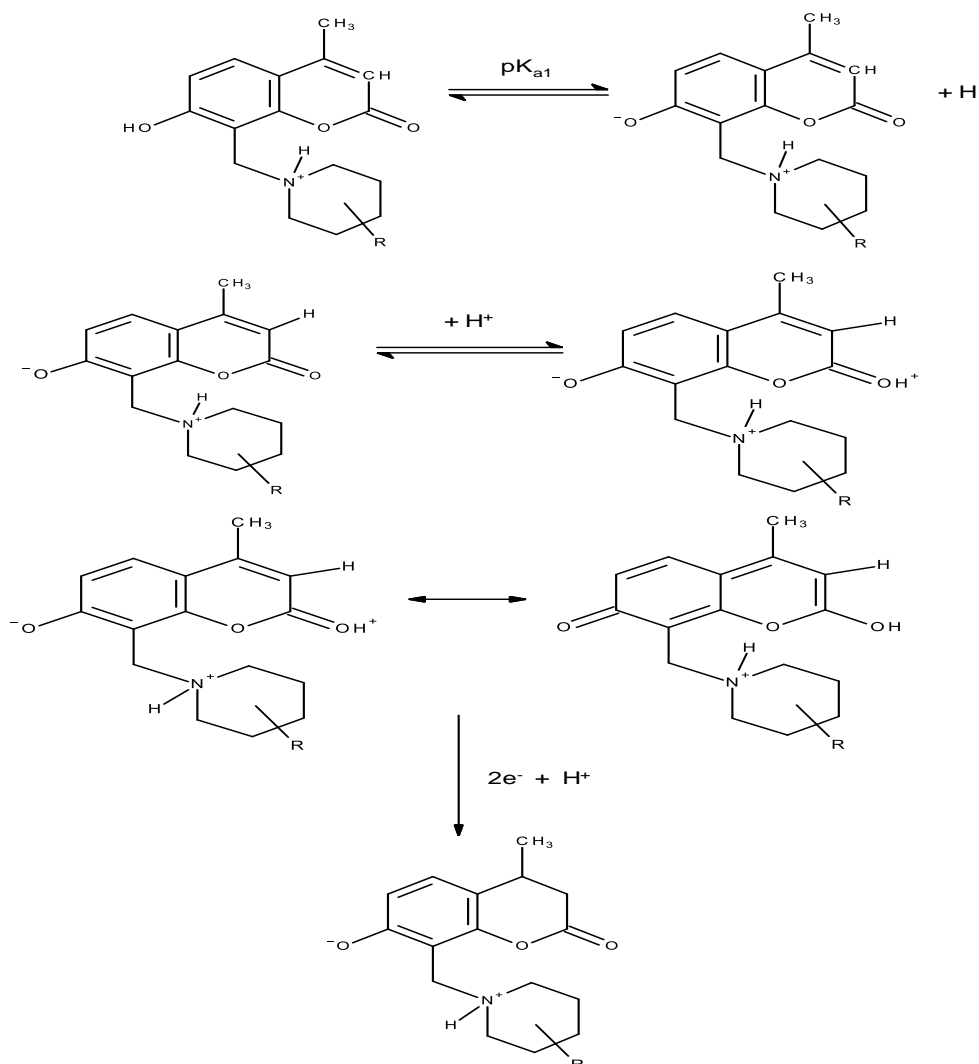
Figure 27.

*E*<sub>1/2</sub>-pH Plot of Compound 24: pH 6.70, pH 7.25, pH 7.70, pH 8.25, pH 8.80



Based on the experimental data and literature, electrochemical reduction mechanism of this group of compounds is suggested in Figure 28.

Figure 28.

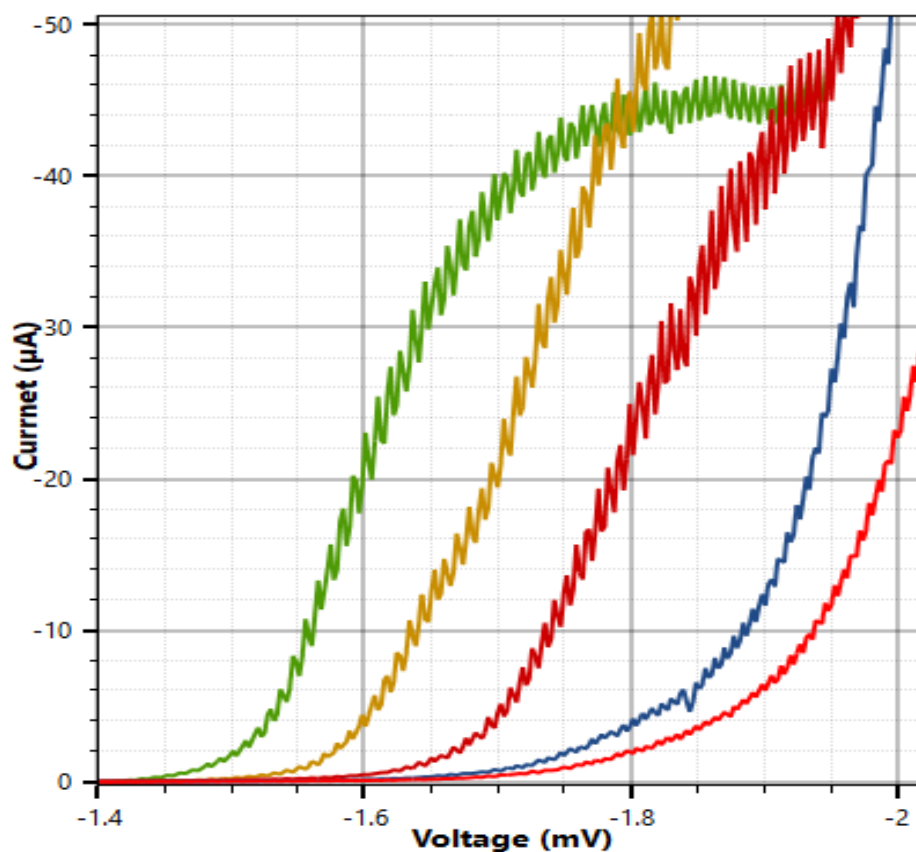
*Electrochemical Reduction Mechanism of Piperidine Derivatives.**Piperazine derivatives*

After we have done working with piperidine derivatives, the electrochemical reduction mechanism of piperazine derivative have been studied. Initially, we have worked with compound **2** and studied to understand the polarographic reduction mechanism in the pH range of 3.70 to 9.80. The concentration of compound **2** was chosen as 0.2 mM at all pH values, and polarographic maxima was suppressed by addition of 1% gelatin in the electrochemical cell. No polarographic curve was found for this compound up to pH value of 7.70. Until pH 7.70, catalytical currents ( $i_c$ ) were observed. This current cannot be used for mechanistic study. After this acidity

value, a peak began to be observed and the current is controlled by diffusion ( $i_d$ ) (figure29).

Figure 29.

*Current-Voltage Plot of Compound 2. pH values: pH 7.70, pH 8.25, pH 8.80, pH 9.25, pH 9.75.*

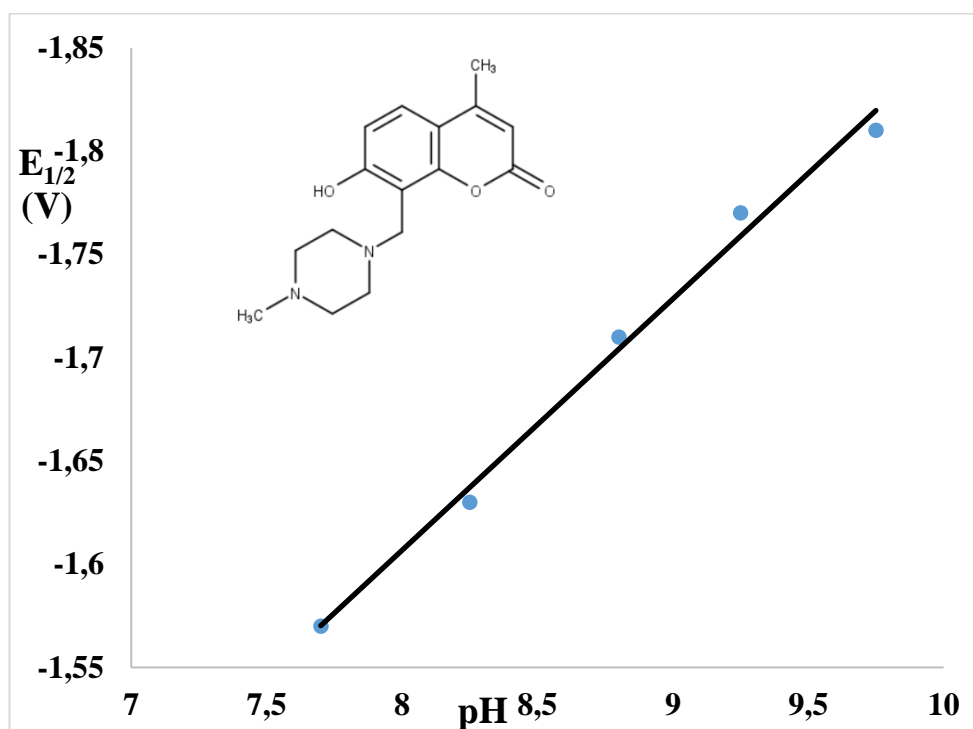


It was observed that the change of  $i$ - $E$  curves depending on acidity did not observe until pH 7.70. It has been seen that the current begins to decrease in more basic solutions. These decreases began to be observed when the pH of the solution is higher than  $pK_{a1}$  value of compound **2** (6.80). In other words, a decrease in current was observed, since the amount of its reducible form decreased when the pH is higher one pH unit than that of  $pK_{a1}$  value. It should be realized that the reducible form, which possesses negative and positive charges, is in the ionized form. Half wave potential value shifts towards a more negative value since the more energy is

required for the reduction of this form. It can be seen from the  $E_{1/2}$ -pH graph (figure 30) when the hydrogen ion concentrations decrease, the reduction potential is shifted to a more negative value.

Figure 30.

$E_{1/2}$ -pH Plot of Compound 2: pH 7.70, pH 8.25, pH 8.80, pH 9.25, pH 9.75.



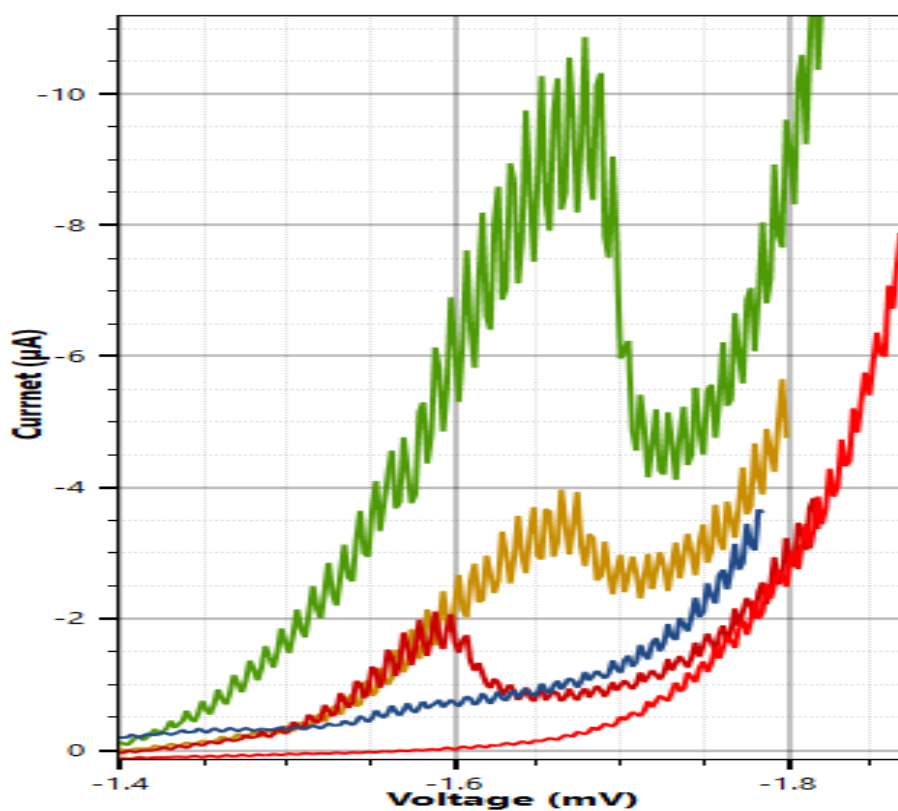
The second acid ionization constant value ( $pK_{a2}$ ) that was found experimentally is greater than 8.80. Therefore, when the acidity of the solution is closer to the second ionization value, the polarographic current-potential curve decreases and no peak is observed after the pH value of 9.75. This shows that the point where the reduction occurs is between two  $pK_a$  values. Therefore, the current that can be observed under reducible conditions was observed in the pH range where negative and positive charges are simultaneously present on compound **2** as piperidine derivatives. Similar behavior was also observed for compound **3**. For these compounds, half-wave potentials depend on the acidity of the solution.  $E_{1/2}$  shifts to more negative values with decreasing acidity of the solution. This result indicates that the hydrogen ion is taken by the compound before the first electron uptakes. This

behavior is similar to reduction mechanism of piperidine derivatives. These compounds contain methyl and ethyl substituents, which are electron donating groups, at the fourth position of piperazine.

After compound **8** (containing electron-withdrawing groups), there is a change in the mechanism of the piperazine derivatives. Acetonitrile was added in the electrochemical cell to increase the solubility of the compound **8**. This compound was studied at all pH values with the addition of 1% gelatin at a concentration of 0.2 mM. 10% acetonitrile was added in the solution. As can be seen from the polarograms (Figure 31), a curve was not observed up to pH value of 6.22. A peak began to be seen at pH 6.70 and disappeared pH around 8.80.

Figure 31.

*Current-Voltage Plot of Compound 8. pH values: pH 6.70, pH 7.25, pH 7.70, pH 8.25, pH 8.80*

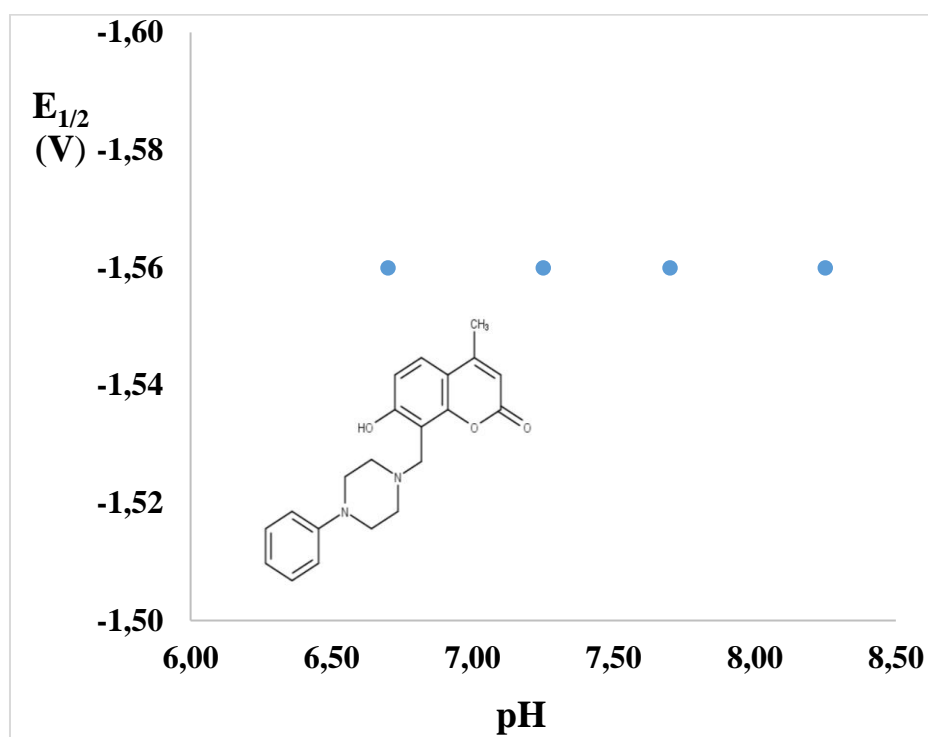


When the pH increased, a decrease in current was observed due to the acidity of the solution is higher than  $pK_{a1}$  value ( $pK_{a1}$  6.63). That means the current decreased because the amount of the reducible form of compound decreased.

It can be seen from the  $E_{1/2}$ -pH plot (figure 32), when the hydrogen ion concentrations decrease, the reduction potentials ( $E_{1/2}$  values) do not shift to a more negative value. This observation tells us that reduction potential is independent of the acidity. This information results in the change in the reduction mechanism.

Figure 32.

*$E_{1/2}$ -pH Plot of Compound 8: pH 6.70, pH 7.25, pH 7.70, pH 8.25*

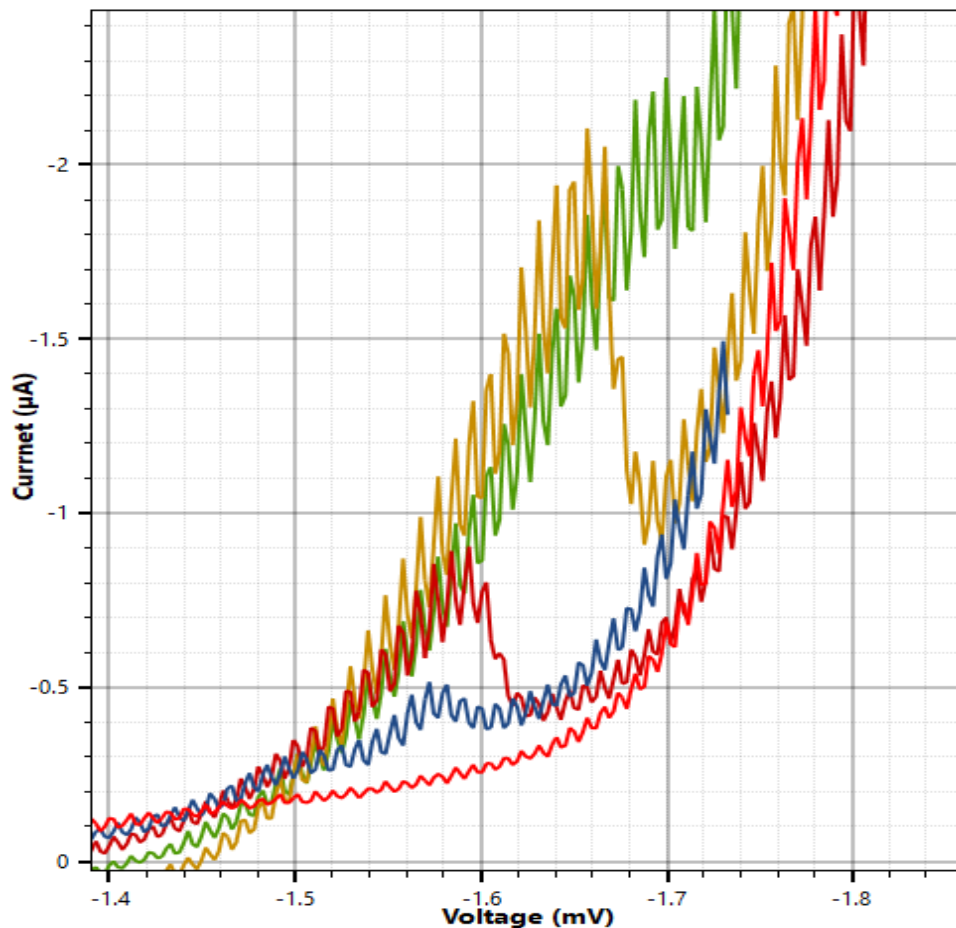


Compound 9 was studied at all pH values with the addition of 1% gelatin at a concentration of 0.2 mM same as other studied compounds. However, due to the decrease in the solubility of compounds, amount of acetonitrile was increased to 20% in the electrochemical cell. As can be seen from the polarograms (Figure 33), a curve was not observed up to pH value of 6.22. A peak began to be seen at pH 6.70 and disappeared pH around 8.80.



Figure 33.

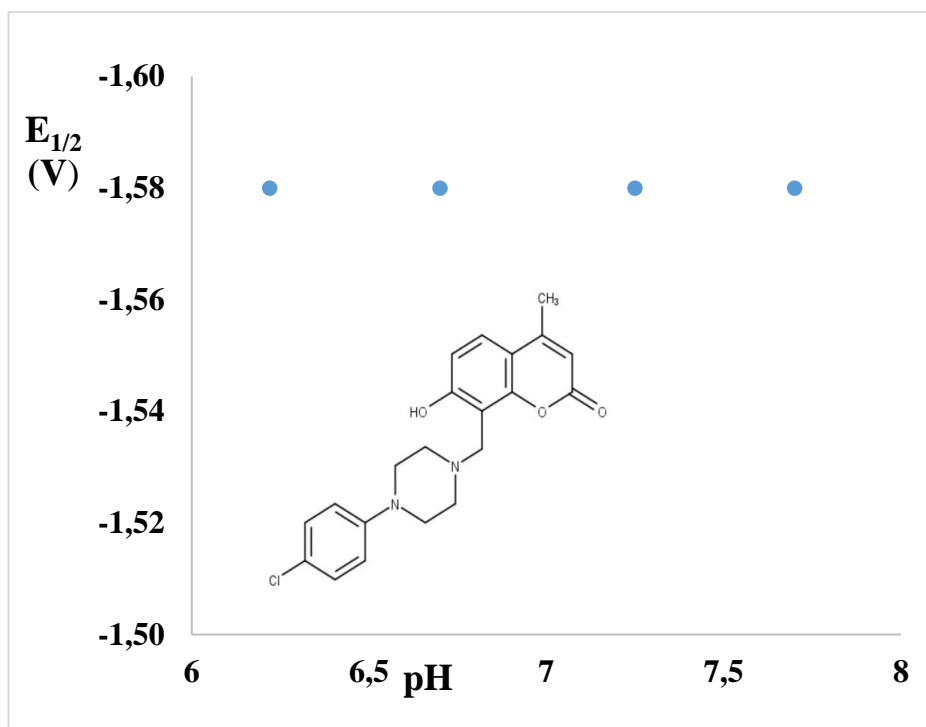
Current-Voltage Plot of Compound 9. pH Values: pH 6.70, pH 7.25, pH 7.70, pH 8.25, pH 8.80



$E_{1/2}$ -pH plot (figure 34) indicates that when the acidity of the cell decreases the reduction potentials ( $E_{1/2}$  values) are independent of the pHs. This plot is similar to compound **8**. This observation shows that there is no hydrogen ion transfer before the first electron uptakes.

Figure 34.

$E_{1/2}$ -pH Plot of Compound 9: pH 6.70, pH 7.25, pH 7.70, pH 8.25



Another studied compound **10** that contains *p*-F-Ph group on piperazine ring. Acetonitrile was added in the electrochemical cell to increase the solubility of the compound **10**. This compound was studied at all pH values (5.80-9.80) with the addition of 1% gelatin at a concentration of 0.2 mM. 20% acetonitrile was added in the solution. As can be seen from the polarograms (Figure35), a curve was not observed up to pH value of 6.22. A peak began to be seen at pH 6.70 and disappeared pH around 9.80.

Figure 35.

Current-Voltage Plot of Compound 10. pH values: pH 6.70, pH 7.25, pH 7.70, pH 8.25, pH 8.80, pH 9.25

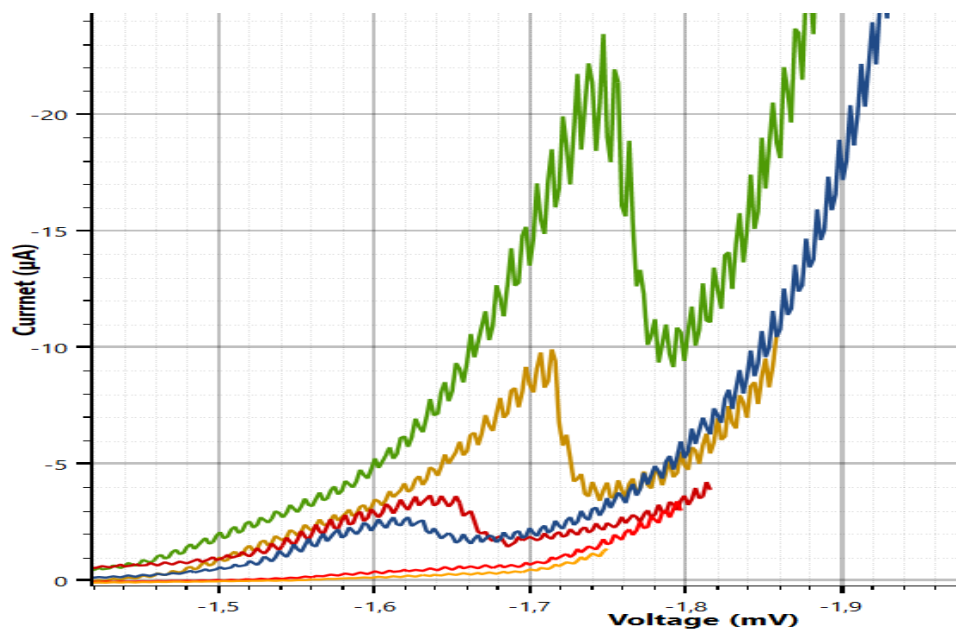
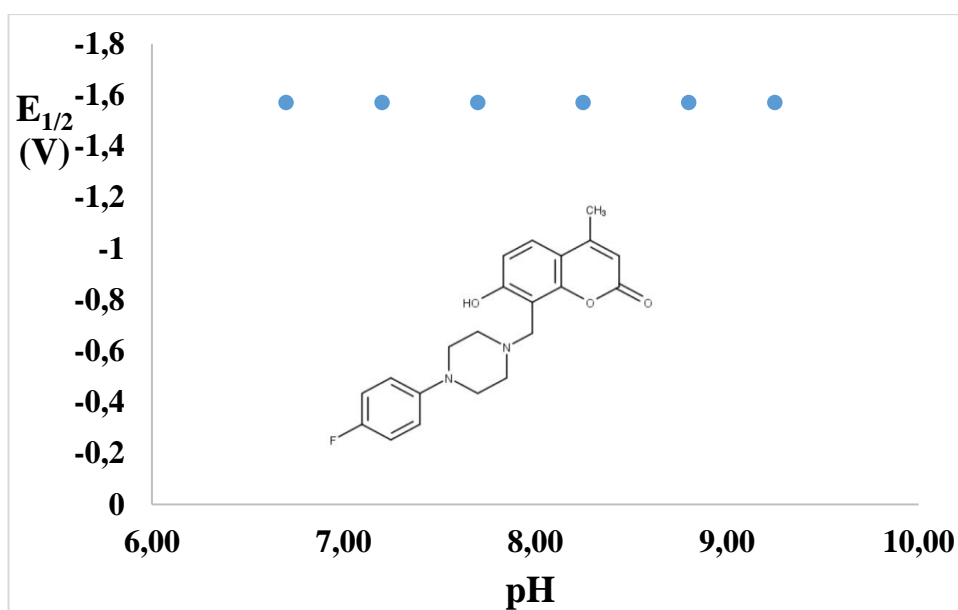


Figure 36.

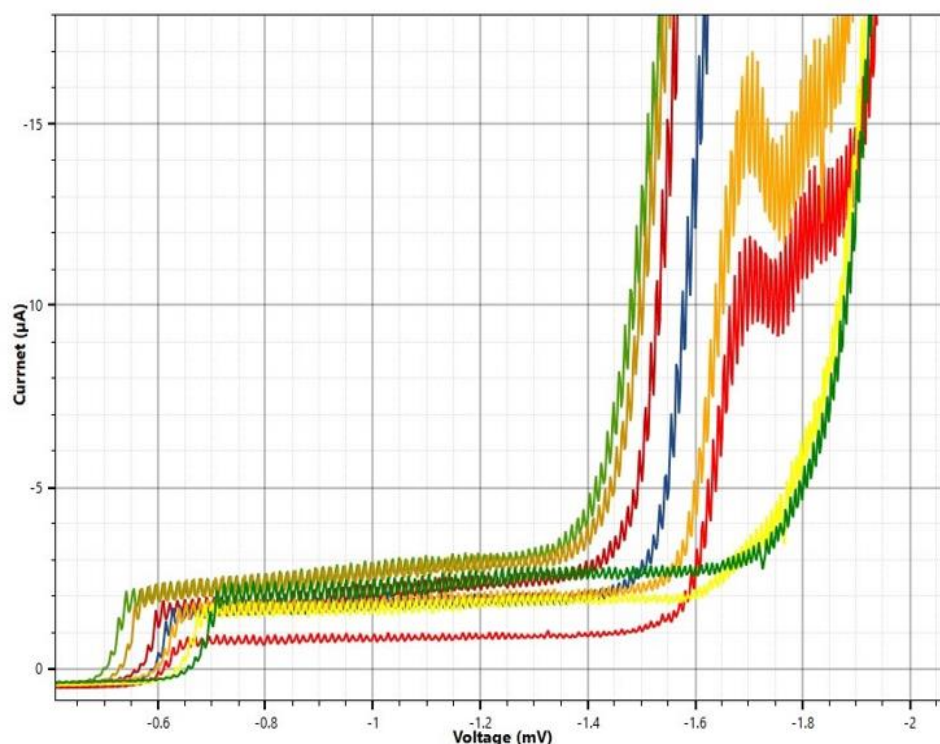
$E_{1/2}$ -pH Plot of Compound 10: pH 6.70, pH 7.25, pH 7.70, pH 8.25, pH 8.80, pH 9.25



As can be seen  $E_{1/2}$ -pH plot (figure 36) shows that when the acidity of the solution decreases the reduction potentials ( $E_{1/2}$ ) are independent of the change in acidity. This plot is similar to compound **8** and **9**. This observation shows that there are no hydrogen ions transfer before the first electron uptakes. Other compounds which contain piperazine ring these are compound **11**, **12**, **13**, **14**, **15** and **16** illustrate same electrochemical behavior with compound **8**, **9** and **10**. However, unlike other substances, the second peak was seen in the polarogram curves of compound **15**, as seen in figure 37. This second peak is due to the reduction of nitro group to amine in the  $-p\text{-NO}_2\text{-Ph}$  group on the piperazine ring.

Figure 37.

*Current-Voltage Plot of Compound 15. pH Values: pH 5,80, pH 6,22, pH 6,70, pH 7,25, pH 7,70, pH 8,25, pH 8,80 pH 9,25.*



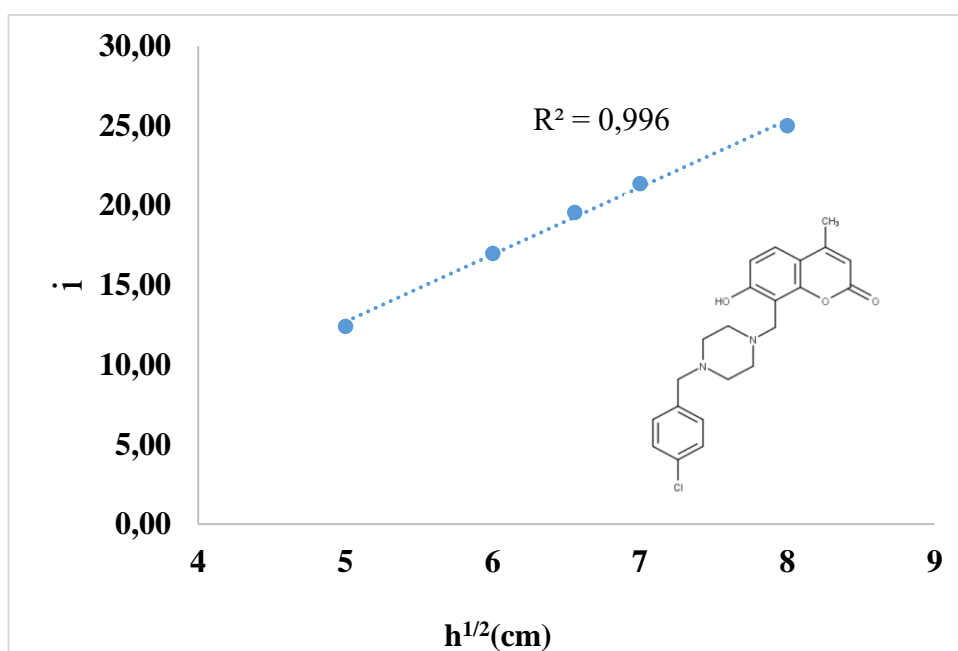
Polarographic currents of organic compounds are in general diffusion-controlled currents, with kinetic currents occurring less frequently. For this reason, it is significant to understand how kinetic currents can be defined. One of the significant evidences of the kinetic current is the dependency on the mercury

pressure. When height of mercury reservoir ( $h$ ) is varied, the height of the kinetic current maintains the same. However, a diffusion controlled current is directly proportional to the square root ( $\sqrt{h}$ ) of the height of the mercury reservoir (P Zuman, 1967).

For compound **11**, polarographic curves were obtained by changing the reservoir height to 25, 36, 43, 49 and 64 cm, respectively, at the same concentration and constant pH of 7.70, and limiting current values were obtained from these curves. Plot of current vs  $h$  can be seen that in Figure 38. The current is proportional with the  $h^{1/2}$ . Hence, for this compound current is controlled by diffusion.

Figure 38.

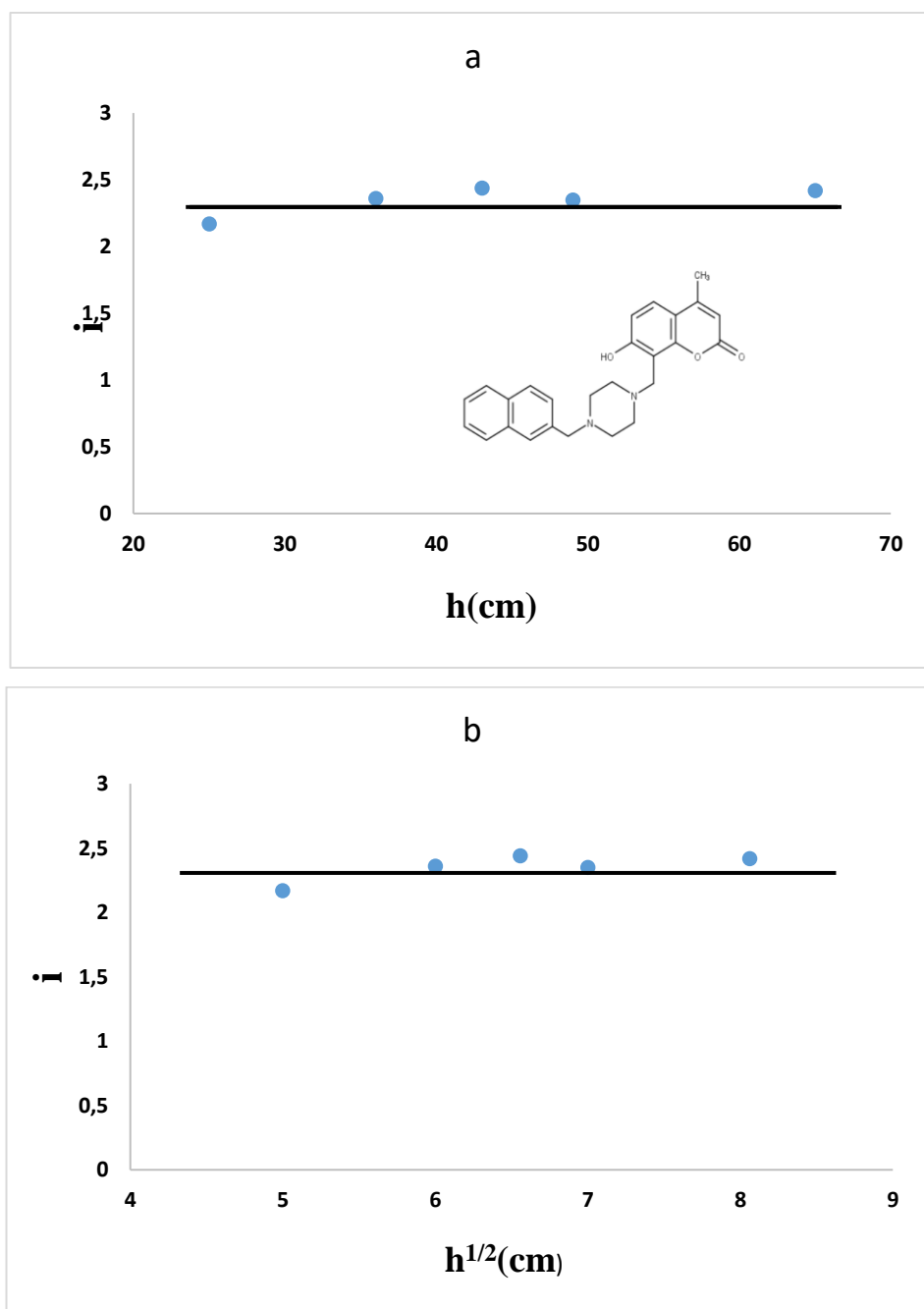
*I-  $h^{1/2}$  Plot of Compound 11*



Another compound **12**, its concentration was 0.2mM and pH of the solution was 9.25. When the mercury reservoir height was varied from 25 cm to 64 cm, respectively, the current was not proportional with the  $h$  and  $h^{1/2}$  as it can be seen in figure 39. Hence, this current was controlled by kinetic.

Figure 39.

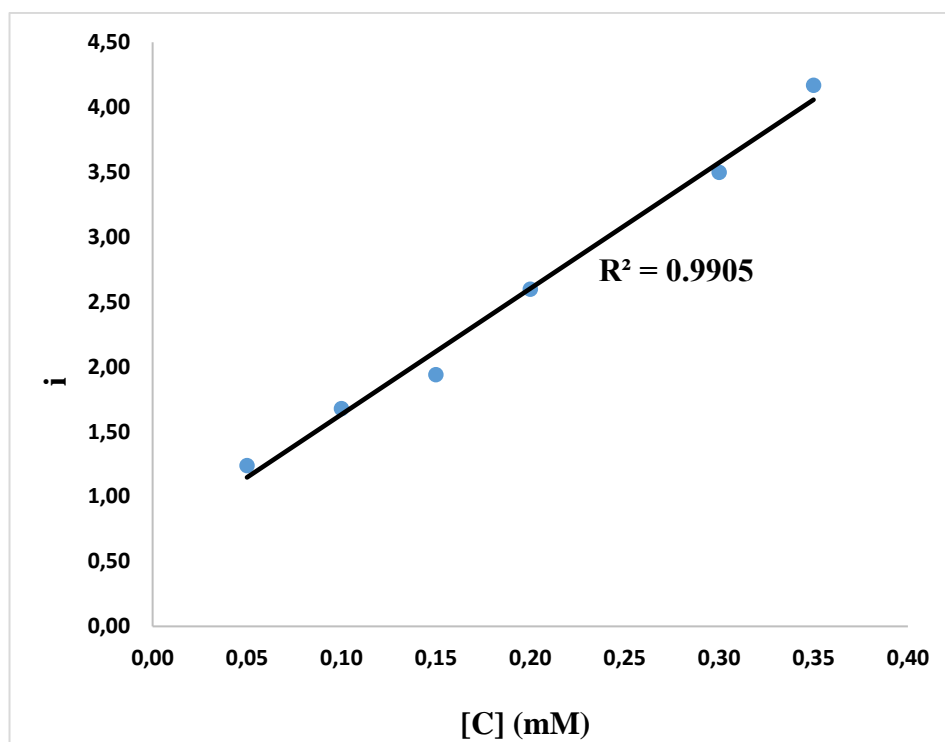
Plot of  $i$  vs  $h$  (a) and  $i$  vs  $h^{1/2}$  (b) for Compound 12



Also, a current is directly proportional to the concentration of the analyte if the current is function of a kinetic reaction (Figure 40). That means the current is controlled by kinetics (P Zuman, 1967).

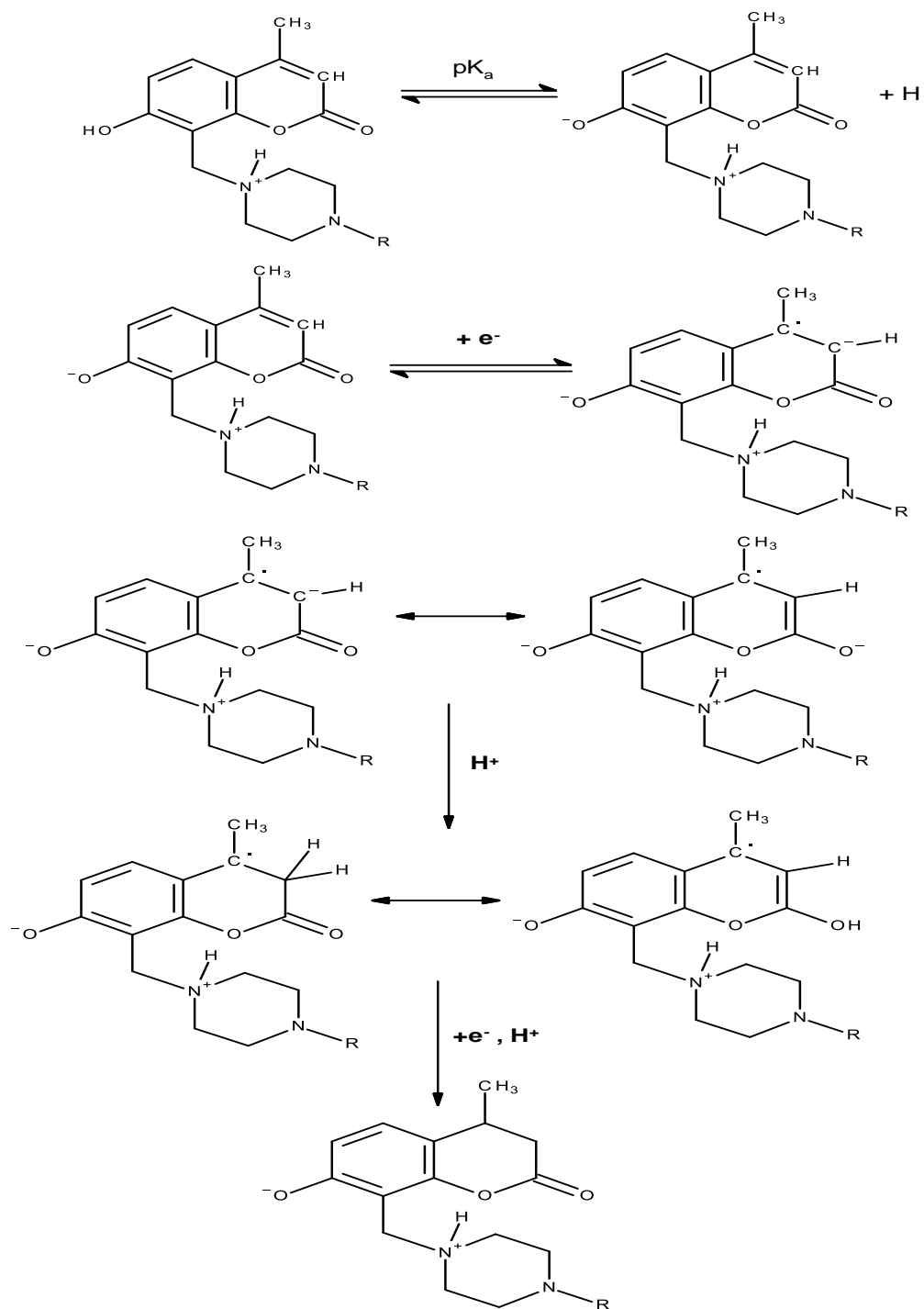
Figure 40.

*Plot of Current vs Concentration for Compound 12*



Based on the experimental data and literature, electrochemical reduction mechanism of piperazine derivatives is suggested in figure 41.

Figure 41.

*Electrochemical Reduction Mechanism of Piperazin Derivatives.*



## CHAPTER V

### Discussion

#### Determination of Ionization Constants

In this study, the ionization constant values of 4-methyl-7-hydroxycoumarin and its derivatives were found by UV-Vis spectrophotometry method and the accuracy of  $pK_a$  values was confirmed by another method, potentiometric titration.

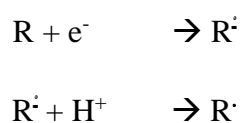
In the literature,  $pK_a$  values obtained for 7-hydroxy-4 methylcoumarin (4MU) molecule were given as 7.80 by UV–VIS spectrophotometry (Mattoo, 1958), 7.91, 7.99 and 7.90 by capillary zone electrophoresis (Nowak et al., 2016), and 7.84 by fluorescence spectroscopy (Moriya, 1983). Experimentally obtained values are in good agreement with the published and theoretically calculated values. Tautomerization of the compound was excluded in the studied pH range as reported in the literature (Moriya, 1983).

If we compare the literature information with the results which we obtained from our thesis study, the experimental  $pK_{a1}$  value of the compound **1** (4-methyl-7-hydroxycoumarin) was 7.91 with the UV-Vis method and 7.95 with the potentiometric method. And these values are similar with literature  $pK_a$  values. According to the literature research, the acid ionization constant values of the other substances which we studied in the thesis have not been found experimentally before. The article containing the studies of the  $pK_a$  values of these substances has been published recently (Erkan Altunterim et al., 2021).

#### Polarography

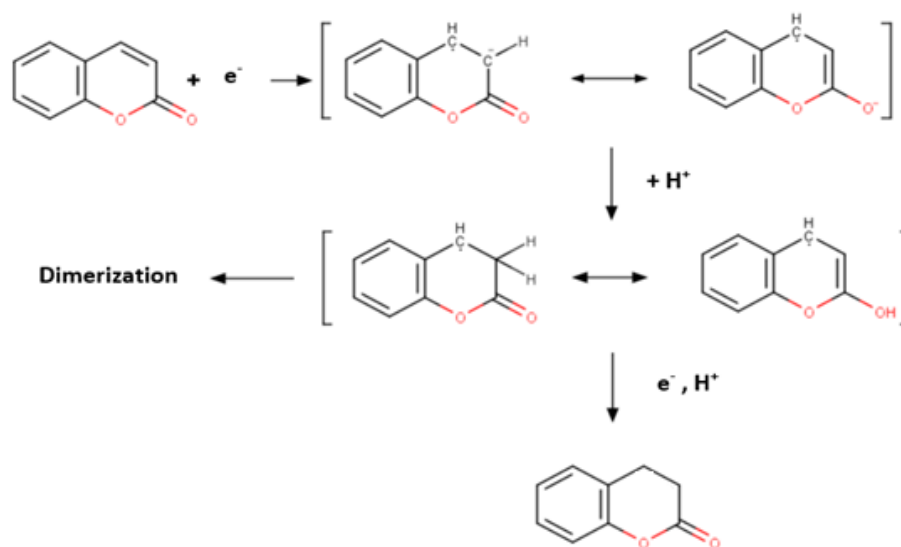
Within the scope of the thesis study, the electrochemical reduction behaviors of coumarin derivatives were investigated. In this context, before studying the two main groups of coumarin derivatives as piperidin and piperazin derivatives, studies in the literature on coumarin and compound **1** were examined, and substance numbered **1** was studied pH between 3.75 and 10.25. Various studies have been carried out on the coumarin substance, which forms the main skeleton of the studied compounds (Dempsey et al., 1993; Gourley, Grimshaw, & Millar, 1970; Harle & Lyons, 1950). In the first study on the coumarin substance by using polarography

(Harle & Lyons, 1950) (Harle and Lyors J.Chem.Soc, 1950, 1575), a single and simple pH independent peak was obtained in the studied pH ranges. They did not observe reduction waves at pH below 4 due to the reduction of hydrogen ions in the supporting electrolyte. Also, it has been reported that half-wave potentials ( $E_{1/2}$ ) were independent of acidity of the solution. Diffusion current ( $i_d$ ) was observed and proven at neutral pH values. In the light of experimental values, based on the fact that  $E_{1/2}$  was independent of pH, it was suggested that electron transfer must have occurred first at least potential determining step and then uptake of hydrogen ions in the reduction mechanism. The reduction mechanism was proposed as follows:



In another study, it was observed that the reduction potentials shifted to a more negative potential than coumarin potential with the substitution of electron withdrawing groups on the main structure of coumarin, which took place in an aprotic medium. The proposed mechanism is as seen in figure 42. With the addition of a single electron to a coumarins, radical and anion forms are formed. With the protonation of these intermediate products, major 4,4'-hydrodimer and a small amount of chroman-2-one are formed as the final products (Pasciak et al., 2015).

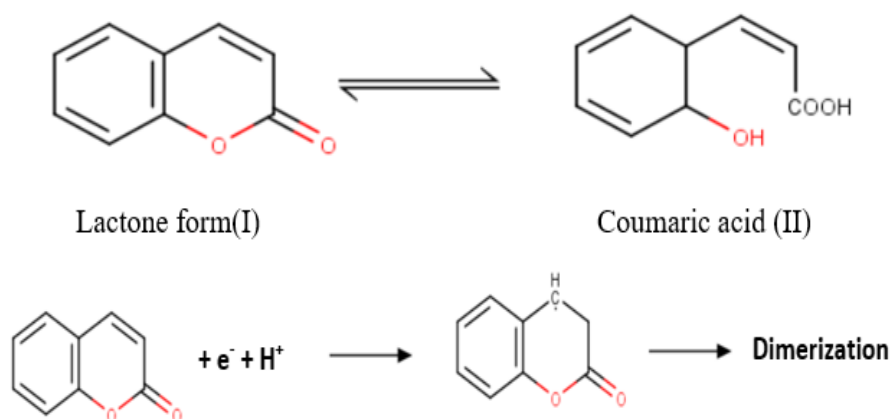
Figure 42.

*Reduction Mechanism of Coumarin*

In a polarographic study of coumarin specification, it was determined that 3,4 double bonds of coumarin were reduced and the reduction potential was -1.56 V. In this study, which was carried out in aprotic environment, it was observed that there were shifts in the reduction potentials of coumarin derivatives obtained by binding different groups on the coumarin main structure. It was determined that the reduction potential shifted to more negative due to the increasing inductive effect with the binding of the electron donating group methyl from the 4-position to the coumarin structure. In the study, it was determined that the reduction potential of 4-OH coumarin was expected to be less than the coumarin reduction potential (-1.56 V) due to the negative inductive effect, but it was reduced at a more negative potential (-1.75 V). They believed this was due to tautomerism. Again, in this study, we saw that the reduction potential of 7-OH coumarin, which is a structure similar to the compound **1** we studied, was -1.69 V. However, we can say that there is a difference in the reduction potential between these two structures due to the presence of a methyl group at the 4 positions in compound **1** and the fact that our study was carried out in an aqueous medium. As a result, both the different groups and the positions of these groups on the structure affected the results (Smyth, Ramachandran, Hack, Joyce, & O'Kane, 2006).

In another polarographic study, in which electroreduction of coumarins took place, a solid electrode was used. The average  $dE_{1/2}/dpH$  value of coumarin was found to be 0.057 in acidic medium and 0.0018 V/pH in basic medium, the study performed in the pH 2-12 range as shown by the data. It was stated that as the pH increased, the  $E_{1/2}$  value increased and it was stabilized at  $pH > 8$ . It seems in the  $E_{1/2}$ -pH graph, the  $pK_a$  value of coumarin was 5.87. Also, they observed two reduction peaks of coumarin between pH 5,01-10,01 by differential pulse voltammetry. Coumarins behavior was observed that showed lactone form(I) and coumaric acid (Jones II & Jimenez) are existing meanwhile the range pH is 6,8 to 11,2. At  $pH < 6,8$  coumaric acid and the  $pH > 11,2$  lactone form exists that shown in figure 43. it was stated that there is one electron reduction to a dimer and the process was diffusion controlled. Therefore, they suggested a possible mechanism is shown below in figure 43 (Wang & Liu, 2009).

Figure 43.

*Possible Mechanism of Coumarin*

## CHAPTER VI

### Conclusion and Recommendations

#### Determination of Ionization Constants

Based on the UV–VIS spectrophotometric and/or potentiometric experimental results and the theoretical calculations of newly synthesized coumarin derivatives,  $pK_a$  values for two acid-base equilibria of the studied compounds were obtained and their protonation reaction schemes were proposed in this study. For the piperazine substituted group of compounds there are two nitrogen atoms that are prone to protonation. The protonation of the second nitrogen on the ring that bears the substituent could not be measured because the dissociation constants of two nitrogen atoms could not be distinguished by the experimental methods chosen for this study. The experimentally found  $pK_{a1}$  values and the theoretically calculated ones were comparable. Also, the published  $pK_a$  value for Compound **1** was found to be similar with the value given here in. Whereas the  $pK_a$  values measured experimentally for all the compounds studied show a good agreement within, for piperidine derivatives  $pK_{a2}$  values differed from theoretical values. In order to explain this observation, hypothetical compounds with hydroxyl substituent on the 6<sup>th</sup> position were studied theoretically and compared with the real compounds that bear hydroxyl on the 7<sup>th</sup> position. From this comparison it has been concluded that the proximity of the oxygen atom to the nitrogen of the heterocycle may help for stabilizing the protonated nitrogen via an electrostatic interaction between the unprotonated negatively charged oxygen and the protonated nitrogen.

Another purpose of this work was to get information about the correlation between acidity constants and anti-inflammatory effects of these twenty-six compounds. Such correlation might help developing new drug candidate molecules. It was found that there is no direct correlation between the acidity and activity of these compounds, however, it was realized that the compounds that have higher anti-inflammatory activities bear benzyl moiety on the substituent. The presence of such a functional group may be suggested for the development of new drug candidates with possible anti-inflammatory effects.

## Polarography

Electrochemical reduction mechanism of coumarin derivatives containing piperidine and piperazine substituents have been studied in this thesis. The behavior of these two groups follows two different way of electron transfer. However, the same group has been reduced for both group of compounds.

For piperidine derivatives, the reduction occurs on the carbon-carbon double bond on the coumarin ring. This reduction depends on the acidity of the solution. It has been shown that before electron uptakes, hydrogen ions transfer first on the coumarin ring due to the dependence of half-wave potentials on pHs. The sequence of electron and hydrogen ions follows  $H^+$  and  $e^-$ . After that, transfer of  $H^+$  and  $e^-$  could not be distinguished based on the experimental evidence. Hence, C=C double bond on the coumarin ring is reduced to C-C single bond as suggested in the literature. Also, the reduction potentials of all piperidine containing coumarin derivatives have the similar values with coumarin derivatives. This may also suggest that the C=C double of piperidine derivatives on coumarin ring follow the same reduction pathway as published results for unsubstituted coumarins in the literature. Polarographic reduction waves can be seen for these group of compounds when the acidity of solution is at least around the  $pK_{a1}$  values of OH group on coumarin ring at 7<sup>th</sup> position. Also, the nitrogen on piperidine group is protonated ( $pK_{a2}$ ). Therefore, the reducible form is a zwitterion. Electron delocalization from C=O double to ionized form of hydroxyl group facilities the reduction of C=C double bond. When pH of the solutions increased, the height of the reduction waves decreased. This observation may be correlated with  $pK_{a2}$  values of piperidine derivatives. When the acidity of the solution approached to  $pK_{a2}$ , reduction waves diminished. These results might recommend that protonated form on nitrogen on piperidine ring stabilize the reducible form.

For piperazine derivatives, the reduction occurs on the carbon-carbon double bond on the coumarin ring as piperidine derivatives. This reduction does not depend on the acidity of the solution. It has been shown that half-wave potentials are independent of acidity of the solution. Therefore, before hydrogen ions transfer, first electron uptakes on the coumarin ring due to the independence of half-wave potentials on pHs. The sequence of electron and hydrogen ions follows  $e^-$  and  $H^+$ . After that, transfer of  $H^+$  and  $e^-$  could not be distinguished based on the experimental evidence. However, C=C double bond on the coumarin ring is still reduced to C-C

single bond as suggested in the literature. Also, the reduction potentials of all piperazine containing coumarin derivatives have the similar potential values with piperidine substituted coumarin derivatives. This may also suggest that the C=C double of piperazine derivatives on coumarin ring follow the same reduction pathway as published results for unsubstituted coumarins in the literature.

Polarographic reduction waves can be seen for these group of compounds when the acidity of solution is at least around the  $pK_{a1}$  values of OH group on coumarin ring at 7<sup>th</sup> position. Also, the nitrogen on piperazine group is protonated ( $pK_{a2}$ ). Therefore, the reducible form is a zwitterion. In this case,  $pK_{a2}$  value of piperazine derivatives are higher than that of piperidine ones. Another word  $pK_{a2}$  values of piperazine derivatives are about ten times higher than that of piperidine ones. This results in more positive reduction potentials (around 100 mV) for piperazine derivatives than that of piperidine ones. Still, electron delocalization from C=O double to ionized form of hydroxyl group facilitates the reduction of C=C double bond due to zwitterion form is present in the solution. When pH of the solutions increased, the height of the reduction waves decreased. Nevertheless, this observation may be correlated with  $pK_{a2}$  values of piperazine derivatives. When the acidity of the solution approached to  $pK_{a2}$ , reduction waves diminished. These results might suggest that protonated form on nitrogen on piperazine ring stabilize the reducible form and also result in half-wave potentials are independent of acidity due to the higher  $pK_{a2}$  values.

## REFERENCES

- Abdel-Latif, N. A. (2005). Synthesis and antidepressant activity of some new coumarin derivatives. *Scientia Pharmaceutica*, 73(4), 193-216.
- Alghool, S. (2010). Metal complexes of azo coumarin derivative: synthesis, spectroscopic, thermal, and antimicrobial studies. *Journal of Coordination Chemistry*, 63(18), 3322-3333.
- Babić, S., Horvat, A. J., Pavlović, D. M., & Kaštelan-Macan, M. (2007). Determination of pKa values of active pharmaceutical ingredients. *TrAC Trends in Analytical Chemistry*, 26(11), 1043-1061.
- Bakirhan, N. K., Celik, M. S. B., Celik, H., Uslu, B., & Ozkan, S. A. (2018). Electrochemical Approach on Mechanism of an Oral Progestin in Aqueous Media and its Fully Validated Detection via a Carbon-Metal Based Composite Sensor. *Electroanalysis*, 30(10), 2273-2283.
- Baymak, M. S., Celik, H., Bakirhan, N. K., Uslu, B., & Ozkan, S. A. (2018). Polarographic Investigation of Dienogest. *Journal of The Electrochemical Society*, 165(10), G128.
- Baymak, M. S., Celik, H., & Ozkan, S. A. (2015). The application of differential pulse polarography to the analysis of capecitabine and investigation of its electroreduction mechanism. *Journal of The Electrochemical Society*, 162(6), G29.
- Biryol, İ. (1995). *Analitik Kimya Ders Kitabı*. Ankara: Ankara Üniversitesi Basımevi.
- Buran, K. (2018). *Design synthesis and evaluation of the biological activity of novel coumarin derivatives* (Publication No.535335). [Doctoral dissertation, Yeditepe University]. Ulusal Tez Merkezi.
- Buran, K., Bua, S., Poli, G., Önen Bayram, F. E., Tuccinardi, T., & Supuran, C. T. (2019). Novel 8-substituted coumarins that selectively inhibit human carbonic anhydrase IX and XII. *International Journal of Molecular Sciences*, 20(5), 1208.
- Buran, K., Reis, R., Sipahi, H., & Önen Bayram, F. E. (2021). Piperazine and piperidine-substituted 7-hydroxy coumarins for the development of anti-inflammatory agents. *Archiv der Pharmazie*, e2000354.
- Dempsey, E., O'Sullivan, C., Smyth, M. R., Egan, D., O'Kennedy, R., & Wang, J. (1993). Differential pulse voltammetric determination of 7-hydroxycoumarin in human urine. *Journal of Pharmaceutical and Biomedical Analysis*, 11(6), 443-446.
- Erkan, S. A., Çoban, G., Durmaz, N. A., Buran, K., Bayram, F. E. Ö., & Çelik, H. (2021). Determination of acid dissociation constant (pKa) values of some newly synthesized coumarin derivatives by using spectrophotometric and potentiometric methods. *Fourrages*, 246(6), 112-141.
- Fais, A., Corda, M., Era, B., Fadda, M. B., Matos, M. J., Santana, L., . . . Delogu, G. (2009). Tyrosinase inhibitor activity of coumarin-resveratrol hybrids. *Molecules*, 14(7), 2514-2520.
- Golfakhrabadi, F., Abdollahi, M., Ardakani, M. R. S., Saeidnia, S., Akbarzadeh, T., Ahmadabadi, A. N., . . . Khanavi, M. (2014). Anticoagulant activity of isolated coumarins (suberosin and suberenol) and toxicity evaluation of *Ferulago carduchorum* in rats. *Pharmaceutical biology*, 52(10), 1335-1340.



- Gourley, R., Grimshaw, J., & Millar, P. (1970). Electrochemical reactions. Part VIII. Asymmetric induction during the reduction of coumarins modified by the presence of tertiary amines. *Journal of the Chemical Society C: Organic*(17), 2318-2323.
- Harle, A., & Lyons, L. (1950). The polarographic reduction of some heterocyclic molecules. Part II. Coumarin and certain derivatives thereof. *Journal of the Chemical Society (Resumed)*, 1575-1578.
- Harvey, D. (2013a). Determining an Acid Dissociation Constant from a Titration. Retrieved from <https://community.asdlib.org/imageandvideoexchangeforum/2013/07/25/determining-an-acid-dissociation-constant-from-a-titration/>
- Harvey, D. (2013b). Mercury Electrodes. Retrieved from <https://community.asdlib.org/imageandvideoexchangeforum/2013/07/31/mercury-electrodes/>
- Harvey, D. (2019). [*eTextbook*] *Analytical Chemistry 2.0*: BCCampus.
- Heyrovský, J., & Zuman, P. (2013). *Practical polarography: an introduction for chemistry students*: Elsevier.
- Jagtap, A. R., Satam, V. S., Rajule, R. N., & Kanetkar, V. R. (2009). The synthesis and characterization of novel coumarin dyes derived from 1, 4-diethyl-1, 2, 3, 4-tetrahydro-7-hydroxyquinoxalin-6-carboxaldehyde. *Dyes and Pigments*, 82(1), 84-89.
- Jones II, G., & Jimenez, J. A. C. (2001). Azole-linked coumarin dyes as fluorescence probes of domain-forming polymers. *Journal of Photochemistry and Photobiology B: Biology*, 65(1), 5-12.
- Keser, G. (1996). *Çeşitli materyallerde diferansiyel puls polarografik yöntemle nitrit miktar tayini [Yayın no 57553]*. (Yüksek Lisans Tezi, Yıldız Teknik Üniversitesi).Ulusal Tez Merkezi.
- Kitamura, N., Fukagawa, T., Kohtani, S., Kitoh, S.-i., Kunitomo, K.-K., & Nakagaki, R. (2007). Synthesis, absorption, and fluorescence properties and crystal structures of 7-aminocoumarin derivatives. *Journal of Photochemistry and Photobiology A: Chemistry*, 188(2-3), 378-386.
- Kulkarni, A., Patil, S. A., & Badami, P. S. (2009). Synthesis, characterization, DNA cleavage and in vitro antimicrobial studies of La (III), Th (IV) and VO (IV) complexes with Schiff bases of coumarin derivatives. *European Journal of Medicinal Chemistry*, 44(7), 2904-2912.
- Lee, Y., & Hu, C. (2014). Mercury drop electrodes. *Encyclopedia of Applied Electrochemistry*.
- Luchini, A. C., Rodrigues-Orsi, P., Cestari, S. H., Seito, L. N., Witacenis, A., Pellizzon, C. H., & Di Stasi, L. C. (2008). Intestinal anti-inflammatory activity of coumarin and 4-hydroxycoumarin in the trinitrobenzenesulphonic acid model of rat colitis. *Biological and Pharmaceutical Bulletin*, 31(7), 1343-1350.
- Mäntele, W., & Deniz, E. (2017). UV–VIS absorption spectroscopy: Lambert-Beer reloaded.
- Matos, M. J., Vazquez-Rodriguez, S., Santana, L., Uriarte, E., Fuentes-Edfuf, C., Santos, Y., & Muñoz-Crego, A. (2013). Synthesis and structure-activity relationships of novel amino/nitro substituted 3-aryl coumarins as antibacterial agents. *Molecules*, 18(2), 1394-1404.
- Mattoo, B. (1958). Dissociation constants of hydroxy coumarins. *Transactions of the Faraday Society*, 54, 19-24.

- Mihaylov, T., Trendafilova, N., Kostova, I., Georgieva, I., & Bauer, G. (2006). DFT modeling and spectroscopic study of metal–ligand bonding in La (III) complex of coumarin-3-carboxylic acid. *Chemical Physics*, 327(2-3), 209-219.
- Moriya, T. (1983). Excited-state reactions of coumarins in aqueous solutions. I. The phototautomerization of 7-hydroxycoumarin and its derivative. *Bulletin of the Chemical Society of Japan*, 56(1), 6-14.
- Murata, C., Masuda, T., Kamochi, Y., Todoroki, K., Yoshida, H., Nohta, H., . . . Takadate, A. (2005). Improvement of fluorescence characteristics of coumarins: syntheses and fluorescence properties of 6-methoxycoumarin and benzocoumarin derivatives as novel fluorophores emitting in the longer wavelength region and their application to analytical reagents. *Chemical and Pharmaceutical Bulletin*, 53(7), 750-758.
- Murray, R. D. H., Méndez, J., & Brown, S. A. (1982). The natural coumarins.
- Nasr, T., Bondock, S., & Youns, M. (2014). Anticancer activity of new coumarin substituted hydrazide–hydrazone derivatives. *European Journal of Medicinal Chemistry*, 76, 539-548.
- Nilapwar, S. M., Nardelli, M., Westerhoff, H. V., & Verma, M. (2011). Absorption spectroscopy. *Methods In Enzymology*, 500, 59-75.
- Nowak, P. M., Woźniakiewicz, M., Piwowarska, M., & Kościelniak, P. (2016). Determination of acid dissociation constant of 20 coumarin derivatives by capillary electrophoresis using the amine capillary and two different methodologies. *Journal of Chromatography A*, 1446, 149-157.
- Orlov, Y. E., & Prokopenko, A. (1969). The polarography of coumarins in alcoholic-aqueous media. I. *Chemistry of Natural Compounds*, 5(4), 184-188.
- Özcan, A. (2011). Kimyasal Denge. In H. Türk (Ed.), *Genel Kimya* (2 ed., Vol. 1966, pp. 236-255). Eskişehir: Anadolu Üniversitesi Web-Ofset Tesisleri.
- Pasciak, E. M., Rittichier, J. T., Chen, C.-H., Mubarak, M. S., VanNieuwenhze, M. S., & Peters, D. G. (2015). Electroreductive dimerization of coumarin and coumarin analogues at carbon cathodes. *The Journal of Organic Chemistry*, 80(1), 274-280.
- Peng, X.-M., LV Damu, G., & Zhou, H. (2013). Current developments of coumarin compounds in medicinal chemistry. *Current Pharmaceutical Design*, 19(21), 3884-3930.
- Refat, M. S., El-Deen, I. M., Anwer, Z. M., & El-Ghol, S. (2009). Bivalent transition metal complexes of coumarin-3-yl thiosemicarbazone derivatives: Spectroscopic, antibacterial activity and thermogravimetric studies. *Journal of Molecular Structure*, 920(1-3), 149-162.
- Rehman, S. U., Chohan, Z. H., Gulnaz, F., & Supuran, C. T. (2005). In-vitro antibacterial, antifungal and cytotoxic activities of some coumarins and their metal complexes. *Journal of Enzyme Inhibition and Medicinal Chemistry*, 20(4), 333-340.
- Reijenga, J., Van Hoof, A., Van Loon, A., & Teunissen, B. (2013). Development of methods for the determination of pKa values. *Analytical Chemistry Insights*, 8, ACI.S12304.
- Rıdvan Say, Ü. D. U., Mutlu Şahin, Sibel Emir Diltemiz, Adnan Özcan, Arzu Ersöz, Ayça Atılır Özcan.Yücel Şahin. (2009). *Analitik Kimya* (1 ed.). Eskişehir: Anadolu Üniversitesi Web-Ofset Tesisleri.
- Samec, Z. (2002). History of the Ilkovic equation. *Review of Polarography*, 48(3), 200-203.

- Sashidhara, K. V., Rosaiah, J. N., & Narender, T. (2007). Highly efficient and regioselective synthesis of keto-enamine Schiff bases of 7-hydroxy-4-methyl-2-oxo-2H-benzo [h] chromene-8, 10-dicarbaldehyde and 1-hydroxynaphthalene-2, 4-dicarbaldehyde. *Tetrahedron Letters*, 48(10), 1699-1702.
- Sethna, S. M., & Shah, N. M. (1945). The Chemistry of Coumarins. *Chemical Reviews*, 36(1), 1-62.
- Skoog, D. A., West, D. M., Holler, F. J., & Crouch, S. R. (2013). *Fundamentals of Analytical Chemistry*: Cengage learning.
- Smyth, W. F., Ramachandran, V. N., Hack, C. J., Joyce, C., & O’Kane, E. (2006). A study of the analytical behaviour of selected synthetic and naturally occurring coumarins using liquid chromatography, ion trap mass spectrometry, gas chromatography and polarography and the construction of an appropriate database for coumarin characterisation. *Analytica Chimica Acta*, 564(2), 201-210.
- Wang, L.-H., & Liu, H.-H. (2009). Electrochemical reduction of coumarins at a film-modified electrode and determination of their levels in essential oils and traditional Chinese herbal medicines. *Molecules*, 14(9), 3538-3550.
- World, S. g. (2021, December 21). Difference Between Single Beam Spectrophotometer and Double beam UV Vis spectrophotometer. Retrieved from <https://www.smacgigworld.com/blog/difference-single-beam-spectrophotometer-and-double-beam-uv-vis-spectrophotometer.php#>
- Yılmaz, F. (1995). *Çeşitli Materyallerde Diferansiyel Puls Polarografik Yöntemle Nitrit Miktar Tayini*. (Yüksek Lisans Tezi), Yıldız Tekbik Üniversitesi, İstanbul. (57553)
- Yu, T., Zhang, P., Zhao, Y., Zhang, H., Meng, J., & Fan, D. (2009). Synthesis and photoluminescent properties of two novel tripodal compounds containing coumarin moieties. *Spectrochimica Acta Part A: Molecular and Biomolecular Spectroscopy*, 73(1), 168-173.
- Zuman, P. (1967). Polarography and reaction kinetics. *Advances in Physical Organic Chemistry* (Vol. 5, pp. 1-52): Elsevier.
- Zuman, P. (1967). *Substituent effects in organic polarography*: Springer.
- Zuman, P. (2001). Electrolysis with a dropping mercury electrode: J. Heyrovsky's contribution to electrochemistry. *Critical Reviews In Analytical Chemistry*, 31(4), 281-289.
- Zuman, P. (2006). Aspects of electrochemical behavior of aldehydes and ketones in protic media. *Electroanalysis: An International Journal Devoted to Fundamental and Practical Aspects of Electroanalysis*, 18(2), 131-140.